Science of the Total Environment 800 (2021) 149460

Contents lists available at ScienceDirect

Science of the Total Environment

journal homepage: www.elsevier.com/locate/scitotenv

Cardiac dysfunction affects eye development and vision by reducing supply of lipids in fish

Elin Sørhus *, Sonnich Meier, Carey E. Donald, Tomasz Furmanek, Rolf B. Edvardsen, Kai K. Lie

Insititue of Marine Research, Nordnesgaten 50, 5005 Bergen, Norway

HIGHLIGHTS

- Exposure to Oil, Nic and Phe led to craniofacial, spinal and eye deformities.
- Exposure to Phe and Nic eliminated ventricular function.
- All treatments led to altered cholesterol and fatty acid profile.
- Fatty acid metabolism, calcium signaling and phototransduction were among most enriched pathways.
- Insufficient supply of lipids and abnormal signaling resulted in eye deformities.

GRAPHICAL ABSTRACT

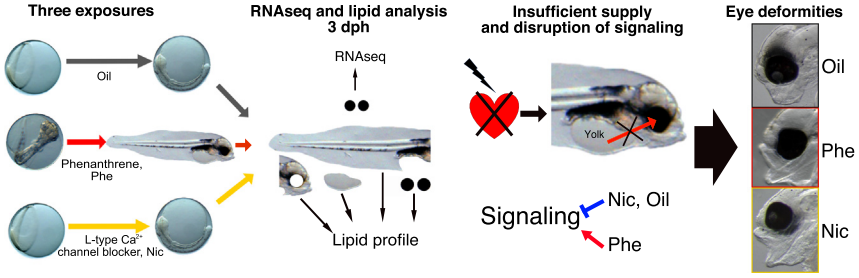

ARTICLE INFO

Article history:
Received 25 May 2021
Received in revised form 31 July 2021
Accepted 31 July 2021
Available online 5 August 2021

Editor: Henner Hollert

Keywords:
Crude oil
Phenanthrene
RNAseq
Lipid profiling
Eye deformities
Early life stages of fish

ABSTRACT

Developing organisms are especially vulnerable to environmental stressors. Crude oil exposure in early life stages of fish result in multiple functional and developmental defects, including cardiac dysfunction and abnormal and smaller eyes. Phenanthrene (Phe) has a reversible impact on cardiac function, and under exposure Phe reduces cardiac contractility. Exposure to a known L-type channel blocker, nicardipine hydrochloride (Nic) also disrupts cardiac function and creates eye deformities. We aimed to investigate whether cardiac dysfunction was the major underlying mechanism of crude oil-, Phe- and Nic-induced eye malformations. We exposed Atlantic haddock (*Melanogrammus aeglefinus*) early embryos to Nic and crude oil (Oil) and late embryos/early larvae to Phe exposure. All three exposures resulted in cardiac abnormalities and lead to severe, eye, jaw and spinal deformities at early larval stages. At 3 days post hatching, larvae from the exposures and corresponding controls were dissected. Eyes, trunk, head and yolk sac were subjected to lipid profiling, and eyes were also subjected to transcriptomic profiling. Among most enriched pathways in the eye transcriptomes were fatty acid metabolism, calcium signaling and phototransduction. Changes in lipid profiles and the transcriptome suggested that the dysfunctional and abnormal eyes in our exposures were due to both disruption of signaling pathways and insufficient supply of essential fatty acids and other nutrients form the yolk.

1. Introduction

Developing organisms are particularly vulnerable to environmental stressors, such as oil pollution. Early life stages of fish are especially susceptible due to their small size, critical developmental window, limited migration capacities, high lipid content and less developed metabolic pathways. It is well known that crude oil exposure causes severe functional and morphometric effects in fish embryo and larval stages (Incardona and Scholz, 2016; Perrichon et al., 2021; Sørhus et al., 2016b). In particular, functional and developmental heart abnormalities, jaw and abnormally shaped eyes and/or reduced eye size have been documented (Incardona and Scholz, 2016; Lie et al., 2019; Perrichon et al., 2021; Perrichon et al., 2018; Sørhus et al., 2021; Sørhus et al., 2017; Sørhus et al., 2016b). Later in life (juveniles and adult stages), these impairments may lead to increased injuries,

* Corresponding author.
E-mail address: elin.sorhus@imr.no (E. Sørhus).

https://doi.org/10.1016/j.scitotenv.2021.149460

developmental delays, changes in swimming capacity and mortality (Cresci et al., 2020; Heintz et al., 1999; Incardona et al., 2015).

Untangling of the underlying mechanisms for these crude oil induced effects has been a focus of research for decades. The heart has been identified as one of the most impacted organs by crude oil exposure, resulting in both morphological and functional phenotypes (Gardner et al., 2019; Incardona and Scholz, 2016). Cardiac function can be directly affected by both crude oil and single polycyclic aromatic hydrocarbons (PAHs), such as phenanthrene (Phe). Both crude oil and Phe interfere specifically with the excitation contraction coupling in cardiomyocytes by disrupting rectifier potassium currents and calcium cycling (Ainerua et al., 2020; Brette et al., 2014; Brette et al., 2017; Kompella et al., 2021). Although it is not clear how Phe disrupts or block various channels, a recent study suggests that Phe acts as an inhibitor of the hERG potassium channel by directly interacting with the channel (Ehab et al., 2021). Exposure to Phe increases intracellular calcium in rat and zebrafish embryonic cardiac myoblasts (Zhang et al., 2013). In addition to its role in the heart, calcium is also a crucial second messenger that is involved in numerous biological functions, like transcription of genes (Newton et al., 2016). Accordingly, the calcium regulated genes were induced by crude oil exposure prior to effects on cardiac function, suggesting that crude oil has a direct effect on calcium homeostasis (Sørhus et al., 2021). Although this direct effect on cardiac function is reversible (Marris et al., 2019), a transient effect on ion homeostasis may disrupt cardiac development and cause irreversible changes in a developing animal (Sørhus et al., 2017). Similarly, a transient disruption of craniofacial muscular function could also irreversibly affect the outgrowth of jaw structures (Shwartz et al., 2012).

Nicardipine hydrochloride (Nic) is a peripheral vasodilator pharmaceutical drug used to treat hypertension, chronic angina pectoris, and Prinzmetal's variant angina (Drugbank.com, 2020). Nic inhibits influx of extra cellular calcium across the membrane, inhibits ion-control gating mechanisms and/or interferes with the release of calcium from internal stores like sarcoplasmic reticulum (Drugbank.com, 2020). The inhibitory action for the calcium channel is limited to the voltage-dependent calcium influxes, and does not affect the receptor operated and NaCl-free-induced calcium influxes (Koide et al., 1983). Thus, by decreasing intracellular calcium, Nic facilitates the relaxation of the muscle cell (Mittnacht et al., 2018).

Exposure to crude oil and oil components have resulted in reduced eye size (anapthalmia) and reduced size with abnormalities (microthalmia) in fish larvae (Lie et al., 2019; Magnuson et al., 2018; Sørhus et al., 2021). Eye development may be affected through several pathways. Vitamin A (retinol) and its biologically active metabolite retinoic acid (RA) plays multiple roles during embryonic eye development (Cvekl and Wang, 2009). Several environmental contaminants, including crude oil and PAHs, have been shown to disrupt RA signaling either through Cyp induction or other Ahr independent pathways (Berntssen et al., 2015; Berntssen et al., 2016; Lie et al., 2019; Williams et al., 2017). Circulatory disorders in early life stages of fish also reduce the eye size (Incardona et al., 2004), suggesting that supply of essential building blocks and nutrients from the yolk is essential for proper eye development. Sufficient amount of the long-chain fatty acids docosahexanoic acids (DHA, 22:6 (n-3)) have been shown to be critical for the developing eye and good visual performance in early larvae stages of marine fish (Bell et al., 1996; Koven et al., 2018; Stoknes et al., 2004).

Previous studies have shown that early embryonic oil exposure (Sørhus et al., 2021) results in cardiac dysfunction and eye deformities. We suspected that associated circulatory disorders may impact lipid distribution in the organism and, in turn, lead to the observed eye malformations. In this study we aimed to link eye abnormalities found after crude oil exposure to heart dysfunction and reduced circulation of essential lipids by comparing crude oil to known cardiotoxic compounds Phe and Nic. The cardiac dysfunction effects of Phe (a component of crude oil) exposure is reversible (Marris et al., 2019), however, ongoing exposure and cardiac dysfunction may be followed by eye deformities. Nic disrupts cardiac contractility specifically by blocking L-type calcium channel. The Nic exposure was included to determine whether disruption of cardiac function alone could introduce eye deformities, while Phe is suspected to have more mechanisms of action. We exposed early embryonic Atlantic haddock (*Melanogrammus aeglefinus*) to crude oil (Oil) and Nic and late embryos/early larvae to Phe. All three treatments led to cardiac abnormalities and severe eye deformities. We measured the distribution of lipids in eyes, yolk sac, head and trunk of the yolk sac larvae and mRNA sequenced the eyes of an additional set of larvae from each exposure. This study provides a better understanding of the underlying mechanisms of the eye phenotypes induced by exposure to Oil, Phe and Nic.

2. Methods

2.1. Passive dosing preparation

A method for silicone passive dosing of Phe (Sigma-Aldrich) was adapted from Vergauwen et al. (2015) and Sørensen et al. (2019). Cords of silicone were precleaned by soaking in methanol overnight followed by two washes of ultrapure water and storage in ultrapure water until use. Approximately 1 g of Phe was added to 30–50 mL of methanol (until saturation) to make the loading solution. Silicone cords were added to the methanol loading solutions and allowed to infuse for two days. After loading, the silicone strips were wiped clean of any solid residues, and methanol was removed by three >2-h soaks in ultrapure water. Three days prior to the exposure, the loaded and rinsed silicone strips were placed in the bottom of a 100 mL glass beaker filled with 60 mL autoclaved seawater.

2.2. Animal collection, management and exposure set up

Fertilized eggs were collected from brood stocks of Atlantic haddock kept at the Austevoll Research Station of the Institute of Marine Research, Norway. Eggs were kept in incubators at 8 ± 2 °C before transfer to exposure tanks, 100 mL beakers or 12-well plates. Experiment overview for all exposures is given in Fig. 1.

2.2.1. Oil exposure

Approximately 5000 embryos at 2.5 days post fertilization (dpf) were transferred to two 50 L green plastic experimental tanks with flow of 32 L/h, water temperature of 8.0 °C and 12/12 light/dark regime. The crude oil was a weathered blend from the Troll oil field, and the exposure regime was performed as described in Sørhus et al. (2016b). The exposure lasted for 72 h, from 10% epiboly to 10–20 somite stage (2.5–5.5 dpf) (Fig. 1). Experimental setup consisted of one control tank (0 μg oil/L) and one oil tank (100 μg oil/L).

2.2.2. Phe exposure

Approximately 100 living eggs were transferred to baked glass exposure jars at 8.5 dpf. One jar contained Phe loaded silicone cord and the control contained cord loaded in clean methanol. Exposure lasted until 3 days post hatching (dph), i.e. from two days after first heartbeat to yolk sac larva stage.

2.2.3. Nic exposure

Approximately twenty-five embryos at 2.5 dpf were transferred to 6 replicate wells in a 12 well plate containing either 10 mL clean autoclaved saltwater or autoclaved seawater spiked with 10 μM Nicardipine hydrochloride (Nic) (Cayman Chemical, USA) ($n = 6$, approx. Total number of embryos = 300). An identical setup with un-spiked autoclaved sea water was included as control. The exposure lasted from 2.5 dpf to 5.5 dpf, and the exposure solution was exchanged every day during the exposure. At 5.5 dpf, eggs from all replicates were transferred to a common glass beaker with clean

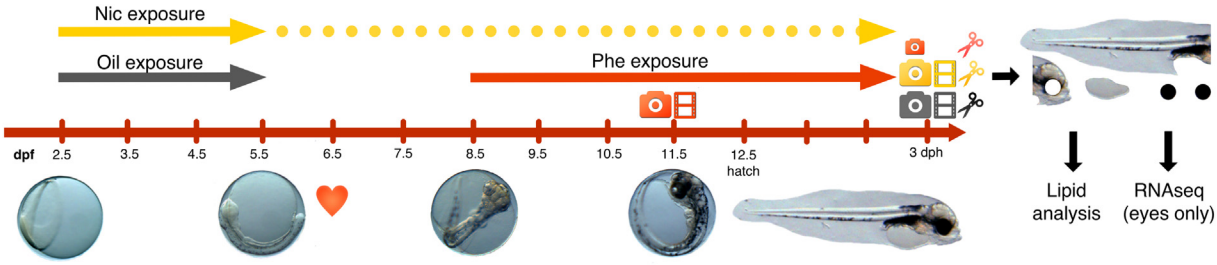

Fig. 1. Experimental overview. Exposure period for the oil (100 μg oil/L) and Nic (10 μM) exposure lasted for 72 h from 2.5 dpf to 5.5 dpf. After exposure the eggs were transferred to clean water, however, Nic binds to a large degree irreversible to L-type calcium channel and therefore the blocking occurs until the sampling point at 3 dph. Phe exposure started at 8.5 dpf to the sampling point at 3 dph. Images and videos were taken at 11.5 dpf for Phe exposure and 3 dph for Oil and Nic. All exposures and associated controls were dissected at 3 dph. Eyes, yolk sac, trunk and head for 10 animals per exposure were subjected for lipid analysis, while eyes from an additional set of animals were subjected for mRNA sequencing. Heart symbol: Time of first heartbeat.

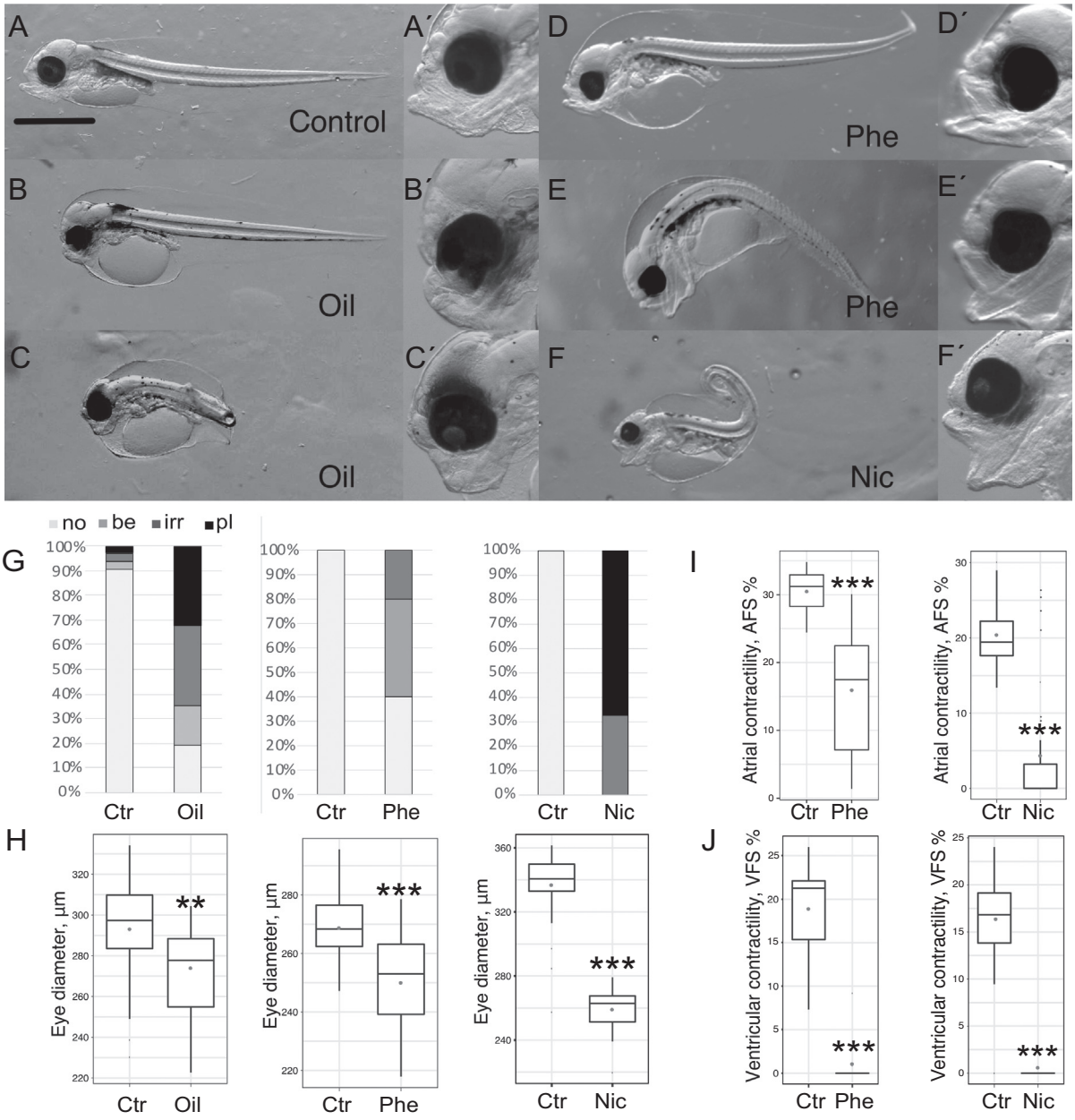

Fig. 2. Phenotypes after exposure to Oil, Phe and Nic. A) Control; B) and C) phenotype after Oil exposure; D) and E) phenotype after Phe exposure; and F) phenotype after Nic exposure. A´) no; D´) bend (be); E´) irregular (irr); B´,C´,F´) protruding lens (pl) phenotype. G) Eye phenotype at 3 dph in 30 (Oil and Nic) and 5 (Phe) individuals. H) Eye diameter at 11.5 dpf (Phe) and 3 dph (Nic and Oil) in μm in 30 individuals. I) Atrial and ventricular contractility or atrial/ventricular fractional shortening (AFS/VFS) in % for Phe and Nic exposure (30 individuals). Statistical differences between exposure and control are indicated by ** ($p < 0.01$) and ***($p < 0.001$).

sea water (one beaker for Nic treated animals and one for control). Water was exchanged every second day until end of experiment (3 dph). The Nic experiment was repeated twice to verify consistency, and the replicate experiments resulted in identical morphological and functional phenotypes.

The exposure scenario for Phe with approximately 200 μg Phe/L (1.12 μM) is not environmentally relevant but chosen to induce an effect. Similarly, the relatively high dose of Nic (10 μM) was given to assure appropriate blocking in the exposure group. The Oil exposure on the contrary, was given an environmentally relevant concentration (100 μg oil/L), reflecting a low to medium exposure in an acute oil spill (Sørhus et al., 2015).

2.3. Analytical chemistry

2.3.1. Oil exposure

Water samples (1 L) were taken from the exposure tanks at the beginning and the end of the experiment (0 h and 72 h), preserved by acidification (HCl, pH < 2) and stored at 4 °C in the dark until further handling. Details are given in Sørensen et al. (2017). Samples for PAH body burden were collected daily during exposure (24 h, 48 h, 72 h) and one day after exposure (96 h). Pooled samples (50–100 animals) were preserved by flash-freezing in liquid nitrogen and stored at −80 °C. *Prior* to analysis, tissue samples were extracted by solid-liquid extraction and cleaned-up by solid phase extraction (SPE).

2.3.2. Phe exposure

Water samples (1.0 mL) were taken for a replicate study performed in the same period and under exact same conditions. These samples were therefore expected to be representative for the Phe exposure in the current study. Samples were collected from three replicate jars immediately before beginning exposures and each day of a three-day exposure period. The water samples were extracted after addition of internal standard using liquid-liquid extraction with two 1 mL volumes of dichloromethane. Water was removed from the extracts with 0.2–0.4 g Na_2SO_4, and extracts were solvent exchanged into isooctane and reduced to 200 μL before analysis on GC–MS/MS.

Agilent 7890 gas chromatograph coupled to an Agilent 7010c triple quadrupole mass detector (GC–MS/MS) was used to perform quantitative analysis of the water samples and body burden. Methods were based on the methods described in Sørensen et al. (2016).

2.4. Morphological and functional measurements

Digital images of un-anesthetized larvae were immobilized in a glass petri dish containing 3% methylcellulose/97% seawater and positioned on a thermally regulated microscope stage (Brook Industries, Lake Villa, IL) at 8 °C. Pictures of 30 individuals were recorded using Moticam 1080 camera (Motic®, Richmond, BC, Canada) mounted on Olympus SZX10 stereomicroscope at 11.5 dpf (Phe) and 3 dph (Nic and Oil exposure). To assess cardiac morphology and function, 20-second videos were captured from 11.5 dpf embryos (Phe) and 3 dph larvae (Nic). Videos were also captured for the Oil exposure, but contractility data from the video analysis of the Oil exposure were rejected because of indications of imaging/sampling related induced stress. Due to low larvae number and no video equipment available at the 3 dph sampling for the Phe experiment, only five representative Phe treated larvae and respective control were photographed at 3 dph using an Olympus SZX10 stereomicroscope equipped with a 5 Mp resolution Infinity camera (Infinity 2–5c, from Lumenera).

Diameter of eye (μm) and ventricular and atrial systolic and diastolic diameters (μm) were processed using imageJ software (Schneider et al., 2012). Atrial and ventricular fractional shortening (FS, %) were then calculated as ((diastole-systole)/diastole)*100. Eye shape phenotypes were described according to the categories: normal (no), bend shape (one indent) (be) irregular shape (two or more indents) (irr) and protruding lens (pl) (see description of eye phenotypes in Sørhus et al. (2021).

2.5. Dissection of 3 dph larvae

Eyes, yolk sac, trunk and head of 3 dph larvae were separated using fine Dumont#55 Forceps (F.S.T. Fine Science Tools) in an Olympus SZX10 stereomicroscope (see Fig. 1). The larvae were anesthetized by adding 500 mg/L MS-222 (Tricaine methanesulfonate, TS 222, Sigma-Aldrich) to a final concentration of 25 mg/L prior to dissection. For RNA-extraction: Three replicates of 10 (Oil and Nic) or 5 (Phe) pair of eyes were either added to RNAlater (Invitrogen) (Oil) or directly to TRIzol reagent (Thermo Fisher Scientific) (Phe and Nic) and kept at −20 °C until total RNA extraction. For lipid analysis: 10 pair of eyes, 8–10 yolk sacs, 10 trunks and 10 heads (with eyes excluded) from each exposure and respective controls were pooled and collected in separate 2 mL glass vials (one tube per tissue type per exposure). The samples were snap frozen in liquid Nitrogen and kept at −80 °C until analysis. The eye diameter used in Table 1 was measured in another representative set of animals at 3 dph (Oil and Nic) and 11 dpf (Phe).

2.6. Lipid analysis

The lipid analysis was performed according to procedures described in detail elsewhere (Meier et al., 2006). In short, the different tissue samples (eyes, yolk sac, trunk and heads) were collected directly into 2 mL glass tubes and the whole sample were analyzed by lipid extraction followed by direct methylation. Thus, no homogenization step was necessary. The samples were extracted with 3 × 1 mL with chloroform:methanol (2:1 *v*/v) and the extract were transferred to 16 mL glass tubes and evaporated to dryness by nitrogen gas, before methylation of all fatty acids to their respective fatty acid methyl esters (FAME). Cholesterol was also extracted and analyzed simultaneously with the FAME. The FAME and cholesterol were analyzed on a HP-7890A gas chromatograph (Agilent, USA) with a flame ionization detector (GC-FID) according to a method described in (Meier et al., 2006) with the fatty acid 19:0 added as an internal standard. 2.5 M dry HCl in methanol was used as a methylation reagent. The FAMEs and cholesterol were extracted using 2 × 2 mL of hexane.

Fatty acids (as 51 FAMEs) were identified by comparing retention times with a FAME standard (GLC-463 from Nu-Chek Prep. Elysian, MN, USA). Retention index maps and mass spectral libraries (GC–MS; http://www.chrombox.org/data) were performed under the same chromatographic conditions as the GC-FID (Wasta and Mjøs, 2013).

2.7. Statistics

Statistical differences in atrial and ventricular contractility and eye diameter were tested using one-way ANOVA with Dunnet's multiple comparison in R (The R Foundation for Statistical Computing Platform) after testing for normality using Shapiro-Wilk test in R. Statistical difference was denoted $p < 0.01$ (**) and $p < 0.001$ (***). Description of statistical analysis of the transcriptome data are found in Section 2.8.

2.8. Extraction of RNA, sequencing and bioinformatics

Extraction of total RNA from the three eye-pools of 10 pair of 3 dph eyes from Oil, Phe and Nic exposures including respective controls was performed using a combination of Trizol/chloroform extraction and Qiagen's RNeasy micro column-based RNA extraction. The material was homogenized in 500 μL TRIzol reagent. Thereafter, 100 μL chloroform (Sigma-Aldrich) was added to each tube, and the tubes were shaken vigorously for 2 min. The samples were incubated at room temperature for 5 min before centrifugation at 10,000 ×*g* for 18 min at 4 °C. After centrifugation the aqueous phase were collected and added to 300 μL 100% ethanol. The samples were transferred to a Qiagen RNeasy

Table 1
Amount of fatty acids and cholesterol (μg/larva) in eyes, head, trunk and yolk from control and exposures groups. C, control; Phe, phenanthrene; Nic, Nicardipine. Single measurements were performed on pools of 10 animals ($N = 1$).

	Total fatty acids (μg/larva)				Cholesterol (μg/larva)			
	Eyes	Head	Trunk	Yolk	Eyes	Head	Trunk	Yolk
Control	0.79	2.93	2.47	1.66	0.12	0.51	0.35	0.07
Oil	0.28	1.37	2.23	1.82	0.04	0.23	0.31	0.08
Oil/C (%)	36%	47%	91%	109%	37%	45%	89%	110%
Control	0.84	2.32	2.78	0.68	0.12	0.42	0.43	0.04
Phe	0.60	2.32	2.70	0.60	0.09	0.40	0.39	0.03
Phe/C (%)	72%	100%	97%	89%	75%	94%	91%	88%
Control	0.660	3.05	2.93	1.630	0.100	0.540	0.480	0.086
Nic	0.45	1.95	3.150	2.010	0.066	0.340	0.490	0.112
Nic/C (%)	68%	64%	108%	123%	69%	63%	102%	130%

Micro column, and the rest of the procedure followed the Qiagen's instructions which also included a DNase I step. The samples were eluted in 15 μL RNase free water.

cDNA library preparation and sequencing were performed by the Norwegian Sequencing Centre (NSC, Oslo, Norway) using the Illumina strand-specific TruSeq RNA-seq library Preparation Kit. A total of 18 samples were sent to the sequencing facility and 16 were subjected for analysis (two samples were lost during cDNA library preparation): Three (Oil/control, Phe/control) and two (Nic/control) biological replicates. Paired-end libraries were sequenced on the Illumina HiSeq 3/4000 platform with read lengths of 150 bp. The raw data are available from the Sequence Read Archive (SRA) at NCBI (Accession ID: PRJNA715613).

Transcriptomic analysis was performed according to previous procedures (Sørhus et al., 2017). For mapping of haddock RNA sequences, we chose to use Atlantic de novo cod trinity transcriptome (Hanna et al., 2020) because the official gene-model versions did not contain full length of all sequences. Of the 39,426 annotated cod reference sequences, there were 34,400 reference sequences with at least 10 mapped haddock reads in one sample. The RNA sequencing data were mapped to the reference sequences of the cod genes (Star et al., 2011) using the Bowtie aligner (RRID:SCR_005476) (Langmead et al., 2009). The mapping efficiency averaged 39%, giving an overall average of 14 million mapped paired end reads (150 bp) for each sample. Transcripts with less than 10 reads in both control and exposure were excluded from further analysis. Mapped reads were normalized to the total number of mapped sequences. Annotation of genes, extraction of number of mapped gene reads (Samstools idxstat), statistics (NOIseqBIO) and Kyoto Encyclopedia of Genes and Genomes (KEGG) pathway analysis was performed as described previously (Sørhus et al., 2017; Sørhus et al., 2016a). Qiagen's Ingenuity Pathway Analysis (IPA version 01–16) was used in addition to KEGG pathway analysis. The log2(fold change) (Log2FC) and p values were extracted from the original NOISeqBIO output. Log2FC values between −1 and 1 was set to 1, as non-significant values and those below 10 reads were originally set to 0.5 and 0.75. Swiss prot IDs were combined with the Log2FC and p-value data and uploaded to IPA. This resulted in 31,376 of 39,426 genes (80%) mapping to the IPA database.

Figures were made using relative regulation of KEGG pathways, i.e. number of genes in pathway divided by number of annotated genes in pathway. Heat maps were generated from Log2(Fold change) data in R (R Core Team, 2013) and Venn diagrams were created using the web-tool, Venn (http://bioinformatics.psb.ugent.be/webtools/Venn). IPA-related figures were extracted directly from the IPA app. To extract most enriched pathways (Canonical pathways and Diseases and Biofunctions) (Fig. 3) an activation z-score threshold of 3 was applied (p-value <0.05). While the p value reflects the likelihood of a pathway being significantly enriched following exposure, the z-score describes the likelihood of a directional association in our dataset. Positive and negative z-scores implies an increase or decrease in activity/activation of the enriched pathway, respectively. z-score > 2 is regarded as significant.

3. Results

Overall, exposure to crude Oil, Phe and Nic resulted in jaw and spinal deformities and smaller and malformed eyes. No ventricular contraction was observed in either Phe or Nic exposure. At 3 dph, changes in fatty acid profile and total cholesterol were found in the eyes of all exposures. Among most affected pathways in the eye transcriptomes were signaling pathways (e.g. *calcium signaling*), muscle function and formation pathways, cholesterol biosynthesis pathways, fatty acid metabolism pathways and phototransduction.

3.1. Exposure

Levels of total PAHs in the Oil exposure were approximately 800 μg PAH/L in water, and approximately 1300 μg PAH/g in tissue at exposure stop. Levels of Phe in the water in the Phe exposure were approximately 200 μg Phe/L. Detailed results are in Supplementary Table 1 and Supplementary Data 1 and 2.

3.2. Morphological and functional phenotypes

Body axis deformities at 3 dph were detected in all exposures. Hunched spine was observed in approximately 50–60% of the Phe treated animals (Fig. 2E), while arched spines and spinal curvatures were seen in all Nic (Fig. 2F) and 53% of the Oil treated animals (Fig. 2B). Similarly, outgrowth of the jaws was affected in all exposures. While a homogenous pool of animals with similar jaws were found in the Nic exposure (Fig. 2F´), Phe exposure showed animals with jaw deformities similar to Nic animals (Fig. 2E´) and animals with less severe jaw phenotypes (Fig. 2D´). The jaw phenotypes in Oil exposure were severe and more undefinable in many of the animals (Fig. 2B´and 1C´) but did not resemble observations in Phe and Nic exposure.

The epithelium of the eye appeared to be thinner in all treated animals opposed to the control animals, and often ruptured during dissection. Abnormal eye phenotypes were seen in all exposure. Images of the eye phenotypes normal, bend, irregular and protruding lens are documented in Fig. 2A´-1F´. The most severe phenotype, protruding lens (pl), was only observed in Oil (32%) and Nic (62%) exposures (Fig. 2G). Eye diameter was significantly reduced in all exposures (Fig. 2H), and the reduction was largest in the Nic exposure.

Exposure to Phe acutely affected cardiac contraction and little to no activity was observed during exposure. After 72 h of exposure (11.5 dpf, Fig. 1) the atrial activity was variable but significantly decreased, while no ventricular contractility was detected (Fig. 2I). Similarly on the seventh exposure day at 3 dph, very little cardiac activity and no ventricular contraction was observed. After exposure, the eggs were transferred to clean water. However, Nic irreversibly binds to L-type calcium channel

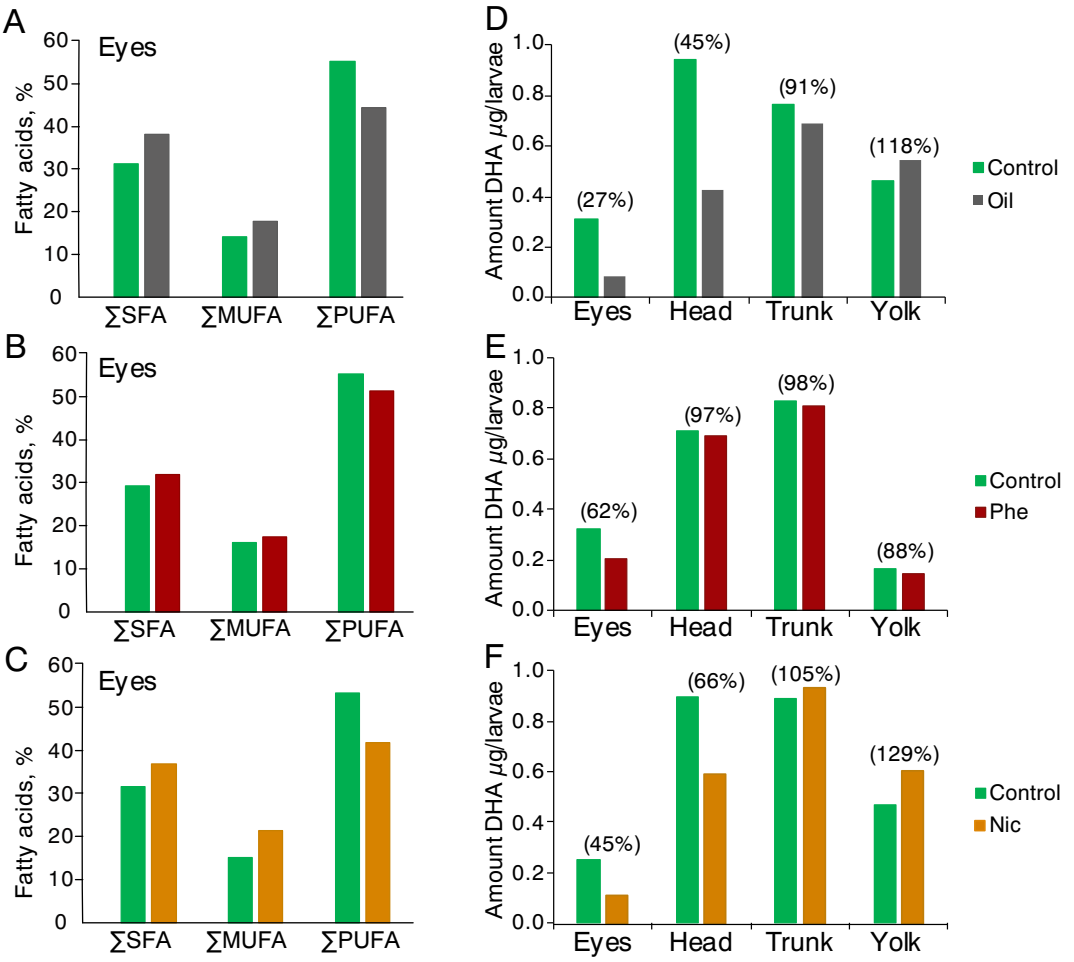

Fig. 3. Distribution of fatty acids. Relative content of saturated, mono- and polysaturated fatty acids in eyes of A) Oil, B) Phe and C) Nic exposures. Amount of docosahexaenoic acid (DHA) (22:6 (n-3)) in eyes, head, trunk and yolk from control and exposure groups; D) Oil, E) Phe, F) Nic. Single measurements were performed on pools of 10 animals. The number in the bracket represents the amount of DHA in the exposure groups relative to their controls (in %).

and therefore blocking occurred up to the sampling point at 3 dph. Very little or no cardiac activity was observed after the expected onset of first heartbeat (6.5 dpf) one day after transfer to clean water until 3 dph (Fig. 2I and J). Contractility data for the Oil exposure were not available.

3.3. Distribution of lipids in 3 dph larvae

The distribution of lipids and lipid profiles were affected in Oil, Phe and Nic exposures (Table 1, Fig. 3, Supplementary Tables 2–4). Total fatty acids and cholesterol were decreased in the eyes both in total amount per larvae but also after normalizing to the eye diameter (Supplementary Table 5). In the eyes of all exposures, the FA profile (% of total FAs) showed higher relative amount of saturated- and monounsaturated fatty acids (ΣSFA and ΣMUFA) while polysaturated fatty acids (ΣPUFA) were lower (Fig. 3A, B and C). Especially, 16:0, 18:0, 18:1 (n-9) and 22:6 (n-3) fatty acids were highly affected in the eyes (Supplementary Tables 2–4, Fig. 3D, E, F). The relative 22:6 (n-3) amount were highest in the eyes (38–39% of total FAs in the control fish) compared with the other three compartments (22:6 (n-3) = 29–32% (Head), 29–30% (trunk), 24–29% (yolk) of total FAs). In the control fish, the ratio between 22:6 (n-3)/20:5 (n-3) was 4.4 in the eyes, while the head, trunk and yolk had much lower ratios, 2.9, 2.7, 2.5, respectively (Supplementary Fig. 1). In the eyes of the exposure groups the ratio between 22:6 (n-3)/20:5 (n-3) was lower compared to control; Oil (3.6), Phe (3.4) and Nic (2.7). In addition, only minor differences were detected between the compartments. In the head, trunk and yolk sac, there were no difference in levels of ΣSFA and ΣMUFA in any of the exposures (Supplementary Tables 2–4). Levels of ΣPUFA and especially 22:6 (n-3) were lower in the heads of the Oil and Nic animals, but not in the Phe animals. Similarly, higher content of 22:6 (n-3) in the yolk was only observed in Oil and Nic treated animals (Fig. 3D, E, F, Supplementary Tables 2–4). The lipid samples clustered according to tissue (eyes, head, trunk and yolk sac), except for Nic and Oil exposed eyes (Supplementary Fig. 2). Detailed fatty acid profiles in eyes, head, trunk and yolk sac for the exposures and respective controls are given in Supplementary Table 2 (Oil), 3 (Phe) and 4 (Nic).

3.4. Differentially expressed genes and most enriched pathways in the eyes of 3 dph larvae

Time period and length of exposure and homogeneity in the exposure pools were reflected in number of differentially expressed genes (DEGs) and enriched pathways. Total number of DEGs ($p < 0.05$) with more than 10 transcripts in the Oil, Phe and Nic were 179, 2643 and 11,980, respectively. The Oil exposure was terminated 10 days before dissection, and correspondingly, fewer pathways were affected in the Oil exposed eyes. The direction of regulation in the Oil exposed eyes mainly followed Nic exposed eyes which were also exposed during early embryogenesis (Fig. 1). IPA Canonical Pathways and Diseases and Biofunctions with activation z-score threshold of 3 or more are presented in Fig. 4A and B, while Fig. 4C displays common pathways among top 40 KEGG pathways in Phe and Nic exposed eyes. For top 40 relative

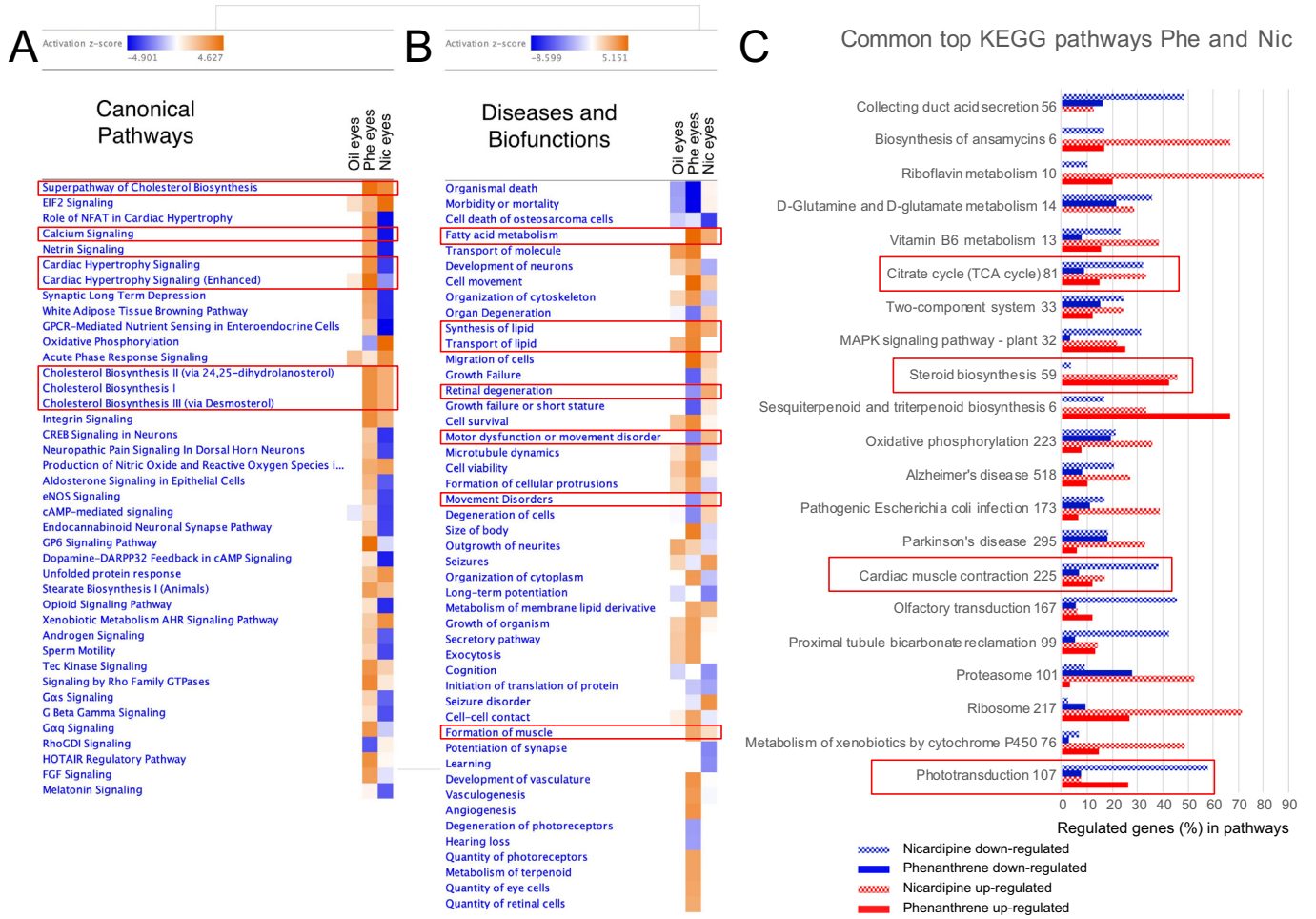

Fig. 4. Top affected IPA and KEGG pathways in eye tissues. Overview of most enriched IPA Canonical pathways (A) and IPA Disease and Biofunctions (B), z-score threshold was set to 3 and *p*-value threshold was set to 0.05. The figure is displayed with z-score. Orange: pathway activated. Blue: pathway inhibited. Darker colors indicate stronger activation/inhibiton. C) Common relative top KEGG pathways for Phe and Nic exposed eyes (Oil exposed eyes were not included due to low number of DEGs). Fold change threshold was set to 1.5 and p-value to <0.05. Number of genes regulated in pathways was divided by number of total annotated genes pathway and are presented as percentage on x-axis. Number behind the Pathway name represents total number of annotated genes in respective pathway. Red and blue bars represent up-regulation and down-regulation, respectively. Outlined pathways: pathways related to fatty acid and cholesterol metabolism, muscle function and formation, calcium signaling and eye development and function. (For interpretation of the references to colour in this figure legend, the reader is referred to the web version of this article.)

KEGG pathways for all exposures, see Supplementary Fig. 3. In general, signaling pathways were activated in the Phe exposed eyes, and inhibited in the Nic exposed eyes (Fig. 4A, Supplementary Fig. 4). Contrarily, IPA *Cholesterol biosynthesis* (Fig. 4A), IPA *Fatty acid metabolism* (Fig. 4B), *Synthesis of lipid* (Fig. 4B), *Metabolism of membrane lipid derivative* (Fig. 4B) and KEGG *Steroid biosynthesis* (Fig. 4C) pathways were activated in both Phe and Nic exposed eyes. Oil exposed eyes also showed an up-regulation of genes in KEGG *Fatty acid biosynthesis* pathway (Supplementary Fig. 3A) in addition to *Transport of lipid* (Fig. 3B). Phototransduction pathway were one of the few other KEGG pathways common for all exposures (Supplementary Fig. 3). Down-regulation was found in Oil and Nic exposed eyes, while mainly an up-regulation was observed in the Phe exposed eyes. Likewise, *Retinal degeneration* (Fig. 4B) was activated in Nic while inhibited in Phe exposed eyes.

3.5. Fatty acid and cholesterol homeostasis

Fatty acid metabolism was among top IPA Diseases and Biofunctions and was activated in both Phe and Nic exposed eyes (Fig. 4B). In the same way, the KEGG pathways *Fatty acid biosynthesis, degradation, elongation, fat digestion and absorption* and *PPAR signaling* were highly regulated, and mainly up-regulated (Supplementary Dataset 3). Several DEGs were shared between *PPAR signaling* and *Fatty acid biosynthesis* and *degradation*. All or most DEGs were exclusive for *Fatty acid elongation* and *Fat digestion and absorption* (Supplementary Dataset 3). Several DEGs involved in the above-mentioned pathways were common for Phe and Nic exposed eyes (Supplementary Dataset 3). Among these DEGs were Fatty acid desaturase 2 (*fads2)* and Fatty acid elongase 6 (*elovl6)* which were up-regulated 2.9 and 3.8 (*fads2)* and 3.2 and 2.9 fold (*evovl6*) in Phe and Nic exposed eyes, respectively (Supplementary Dataset 3). Another *elovl*, *elovl4,* were highly expressed in the eyes regardless of exposure (e.g. *elovl4* (IMR10009452) with approximately 7000 normalized transcripts, Supplementary Dataset 3). However, expression levels were reduced in the Nic exposure (FC = −2.5, 3000 normalized mean transcripts, Supplementary Dataset 3). Upstream regulator indicated reduced levels of *high-density lipoproteins* (HDL), cholesterol, lysophosphatidylcholine and DHA in Nic and Phe exposed eyes, while PPARGC1b and PPARD were increased in the same samples (Supplementary Fig. 5).

Cholesterol pathways were also activated in both Phe and Nic exposed eyes (Fig. 4). A condensed pathway combining *Mevalonate pathway* and *Superpathway of cholesterol* show that almost all genes involved in the pathways were up-regulated (Fig. 5). Interestingly, 3-hydroxy-3-methylglutaryl-CoA reductase (*hmgcr*) and 3-hydroxy-3-methylglutaryl-CoA synthase 1 (*hmgcs1*) were only up-regulated in the Phe exposed eyes. Another interesting gene up-regulated was the TLC domain containing protein 1 (*tlcd1*) which was up-regulated in both Phe and Nic exposure.

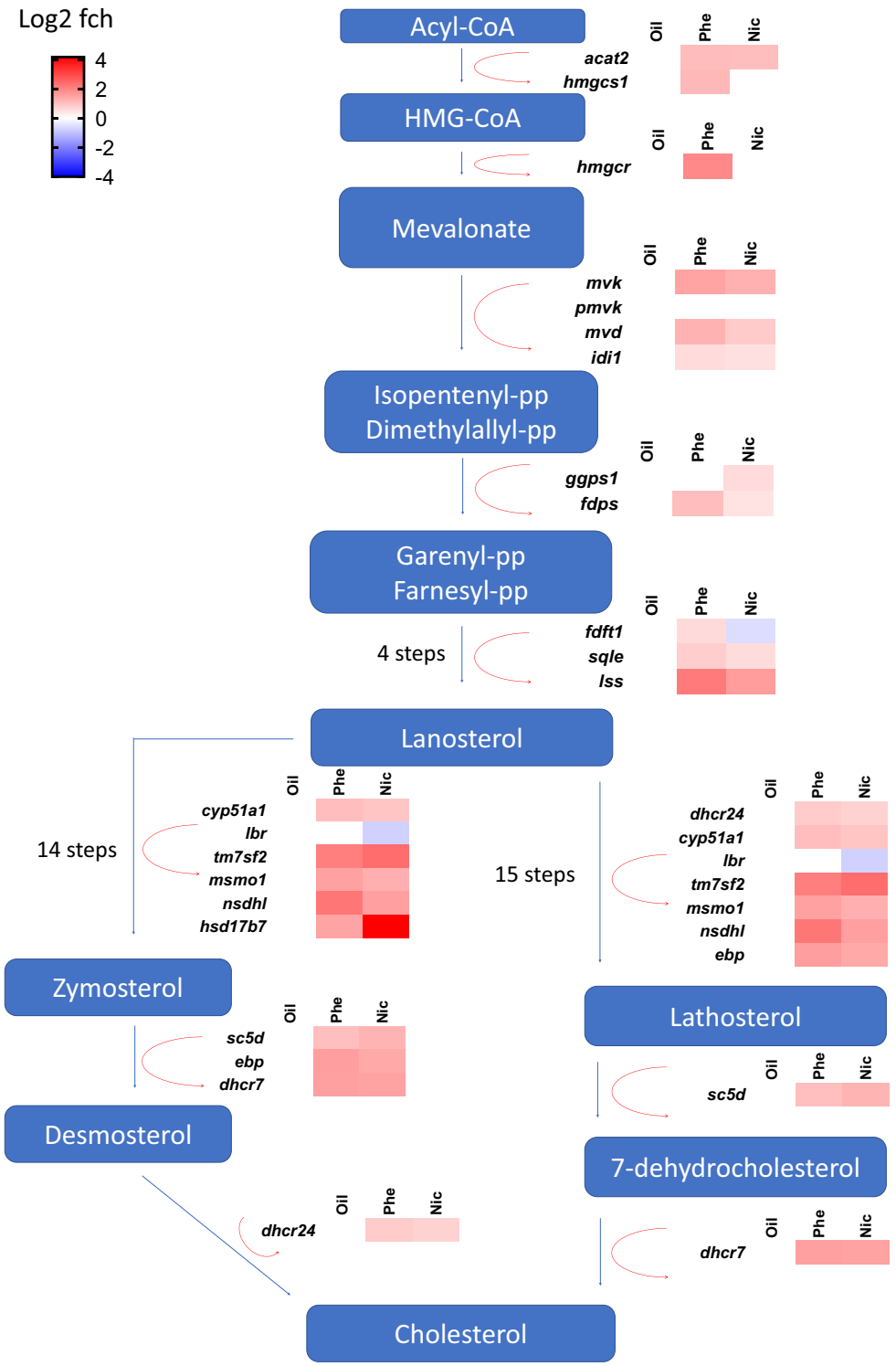

Fig. 5. Superpathway of cholesterol and Mevalonate pathway. Mevalonate pathway and Superpathway of cholesterol combined. Differentially expressed genes indicated as heatmaps next to the respective step. Log2FCH; base 2 logarithm of the fold change.

3.6. Calcium signaling and muscular function

Calcium signaling pathway was among IPA Canonical pathways with highest activation score (Fig. 4A). Only one DEG (*grin1*) was common for all exposures, while we found 28 common DEGs for Phe and Nic exposed eyes (Fig. 6A), but mainly with opposite expression (Fig. 6B). For example, the genes encoding L-type channels (*cacna1f*), skeletal muscle Ryanodine receptor 1 (*ryr1*) and inositol 1,4,5-trisphosphate receptor type 1 (*itpr1*) were up-regulated in Phe exposed eyes and down-regulated in Nic (Fig. 6 and Supplementary Data 4). Oil exposed eyes only had 6 DEGs in *Calcium signaling* pathway, all common to and in the same direction as Nic exposed eyes (Fig. 6C).

Similar to *Calcium signaling* pathway, the Disease and Biofunctions *Motor dysfunction or movement* and *Movement disorders* were oppositely activated in Phe vs Nic. Here, Nic was activated and Phe was inhibited (Fig. 7). A visual web of the DEGs (262) in *Motor dysfunction and*

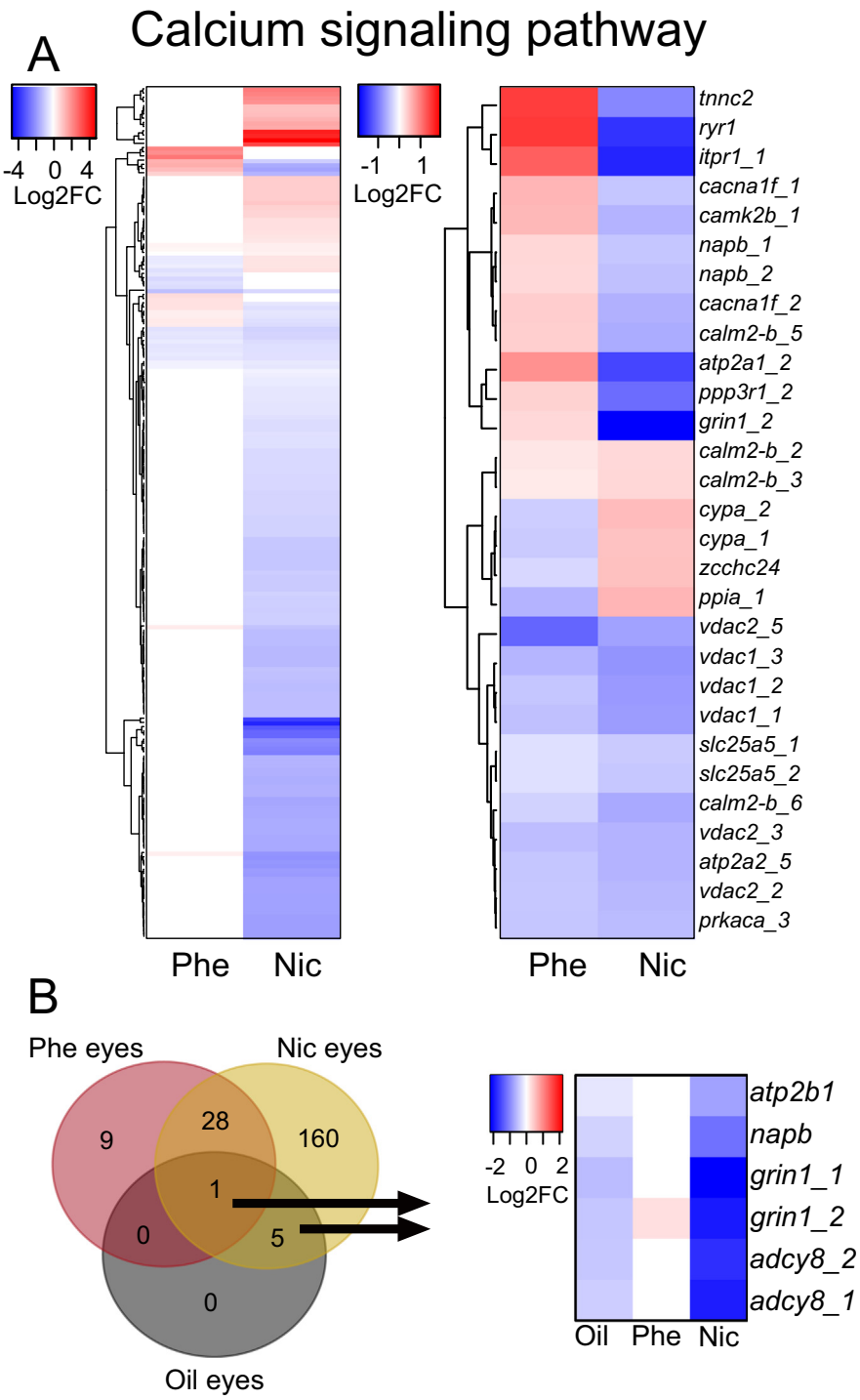

Fig. 6. Calcium signaling pathway. A) KEGG Calcium signaling pathway. Left: All differentially expressed genes (DEGs) in genes in Oil, Phe and/or Nic exposed eyes. Right: DEGs common for Phe and Nic exposed eyes. B) Left: Venn diagram for DEGs in KEGG calcium pathway for all exposures. Right: Heatmap of all DEGs in Oil exposed eyes within KEGG Calcium signaling pathway.

movement disorder in Phe exposed eyes overlapping with the Canonical pathways (CP), *Calcium signaling* (21 genes) and *Cardiac hypertrophy signaling (Enhanced)* (19 genes) are shown in Supplementary Fig. 6A. A complementary web of the same genes for Nic exposed eyes (Supplementary Fig. 6) mainly shows the opposite expression. Similarly, KEGG *Cardiac contraction* pathway, which in this context reflects effect on muscular function in the eyes and not cardiac contraction, was also oppositely regulated in the two exposures (Supplementary Fig. 7, Supplementary Data 5). *Formation of muscle* on the contrary, was activated in both exposures (Fig. 7A). To visualize common DEGs in between some of these pathways, Venn diagrams including IPAs *Calcium signaling*, *Cardiac hypertrophy signaling*, *Motor dysfunction and movement disorders* and *Formation of muscle* were made and are displayed in Fig. 7B. Especially *Calcium signaling* pathway had several DEGs in common with the other pathways. For example, in the Nic exposed eyes, only 19 of 108 DEGs were exclusive for *Calcium signaling* pathway.

3.7. Retinol metabolism and Phototransduction

Retinol metabolism was affected in Phe and Nic exposed eyes but not in Oil exposed eyes. Phototransduction pathway, on the other hand, was affected in eyes for all exposures (Fig. 8).

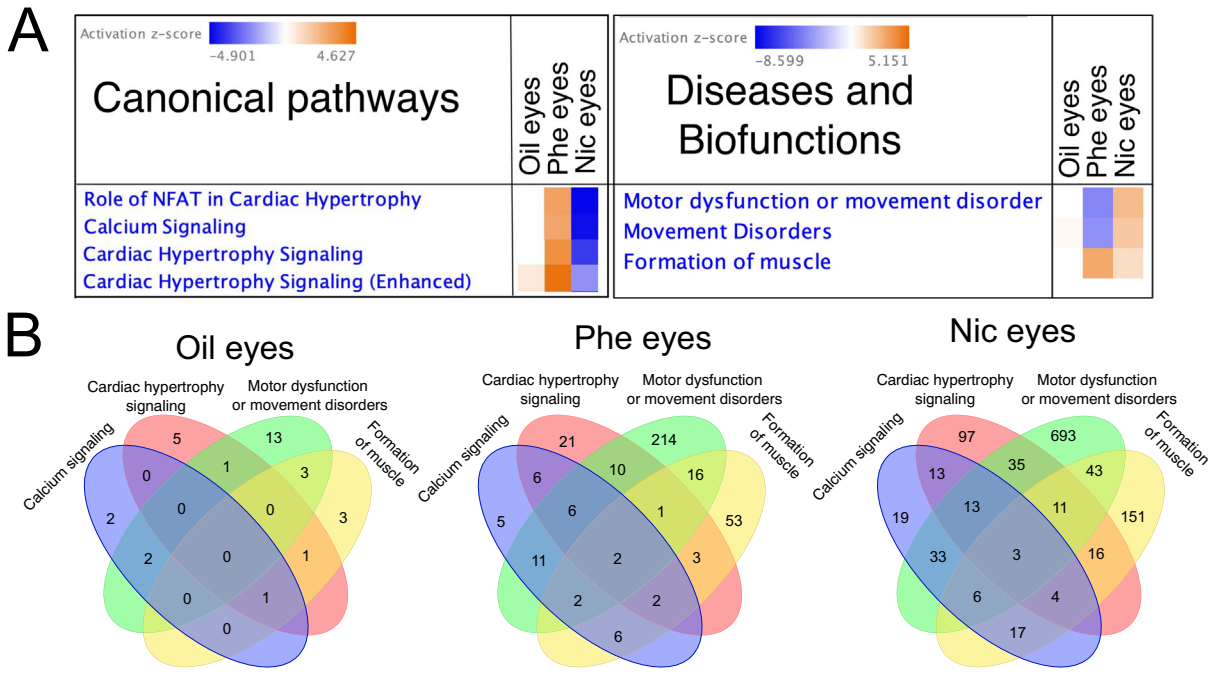

Fig. 7. Calcium signaling pathway, motor dysfunctions and muscle formation. A) IPA z-score tables for selected Canonical pathways and Diseases and Biofunctions. B) Venn diagram showing common differentially expressed genes in IPA Calcium signaling pathway, Cardiac hypertrophy signaling (Enhanced) pathway, and Motor dysfunction or movement disorders and Formation of muscle. Threshold *p*-value for DEGs >0.05.

In *Retinol metabolism*, ten of the DEGs were common for the Phe and Nic exposures (Fig. 8A). Transcripts were mainly up-regulated in Phe exposed eyes, while more variable in the Nic exposed eyes (Fig. 8B). In *Phototransduction* pathway most genes were down-regulated in Nic exposed eyes, while more variable in Phe exposed eyes. Oil exposed eyes had only 12 regulated genes which all were common with findings in Nic exposed eyes (Fig. 8A) and also showed the same direction as Nic exposed eyes (Fig. 8B). Phe and Nic exposed eyes had 30 genes in common (Fig. 8A), and only 8 were regulated in the same direction (Fig. 8B).

4. Discussion

4.1. Exposure

The initial intention for the Nic exposure was to expose in the same developmental period as the Oil exposure (i.e 2.5–5-5 dpf). However, Nic continues to block cardiac function after transfer to clean water, and we suspected that the effect was irreversible. Nic is readily metabolized in the liver with a half-life of 8.5 h in humans (Drugbank.com, 2020). But there is no knowledge on the metabolization rate in the early life stages of cold-water fish species. The haddock embryos do not have fully developed liver until open mouth stage (1 dph) (Hoehne-Reitan and Kjørsvik, 2004), with the rudimental liver cells visible at 7 dpf (Hall et al., 2004) and liver bud appearing approximately at hatch (Sørhus et al., 2016b). Thus, an incomplete metabolism of the drug is likely, resulting in a partly irreversible effect in the developmental period examined.

4.2. Spinal and jaw deformities most likely linked to disruption of skeletal muscle function

The consequences of an exposure are dependent on the exposure length and the developmental period of exposure (Sørhus et al., 2017; Sørhus et al., 2016b). In present study, we found that the Nic exposure gave the most homologous severely malformed population. The morphological phenotypes in the Phe exposure were more variable. However, all animals showed the same functional phenotype, a non-contracting or silent ventricle that demonstrated the acute effect Phe has on cardiac function (Brette et al., 2017; Marris et al., 2019). In the Oil exposure, morphological phenotypes were also variable but more severe, reflecting various impacts from multiple toxicants in the complex oil mixture during an essential period of development (2.5 dpf-5.5 dpf).

Spinal and jaw deformities could be secondary to cardiac dysfunction (Incardona et al., 2004), a result of signal disturbance (mainly in early embryonic development) (Planchart and Mattingly, 2010; Xiong et al., 2008), or a direct effect on muscular function (Goodman et al., 2015; Shwartz et al., 2012). After 72 h of Phe exposure, no ventricular contraction was observed, suggesting a specific impact on cardiac ventricular function. Accordingly, tricyclic PAHs such as Phe are known to impact cardiac function directly (Incardona et al., 2004) by disturbing potassium and calcium currents essential for excitation contraction coupling (ECC) in the cardiomyocytes (Ainerua et al., 2020; Brette et al., 2017; Kompella et al., 2021). Nic blocks the L-type calcium channel and inhibits influx of calcium across the membrane of both myocardial and smooth cells (Mittnacht et al., 2018) and skeletal muscle cells (Sato and Fujino, 1987), although the predominant effect is on arterial smooth muscle cells in humans (Mittnacht et al., 2018). We expected an impact on all muscle fibers in the Nic exposure. However, it is not known whether Phe's impact on ECC is solely reserved for cardiac tissues or would have the same effect in all excitable tissues similar to the Nic exposure. Appropriate outgrowth of jaws is dependent on craniofacial muscle function (Shwartz et al., 2012), and therefore paralyzing craniofacial muscles would result in similar abnormalities observed in the present study. In addition, Nic and Oil animals were exposed during organogenesis, potentially affecting development of craniofacial elements (Knight and Schilling, 2006). Interestingly, despite that Phe was exposed in late organogenesis, the Nic craniofacial phenotypes resemble the Phe phenotypes more than Oil phenotypes. This suggests that opposed to Oil exposure, Nic exposure do not seem to affect patterning of jaw but only affect outgrowth of the jaws.

There is a close interdependent development of the spinal cord and muscle fibers along the cord (Stifani, 2014). A direct effect on skeletal muscle fibers could potentially result in the spinal abnormalities seen

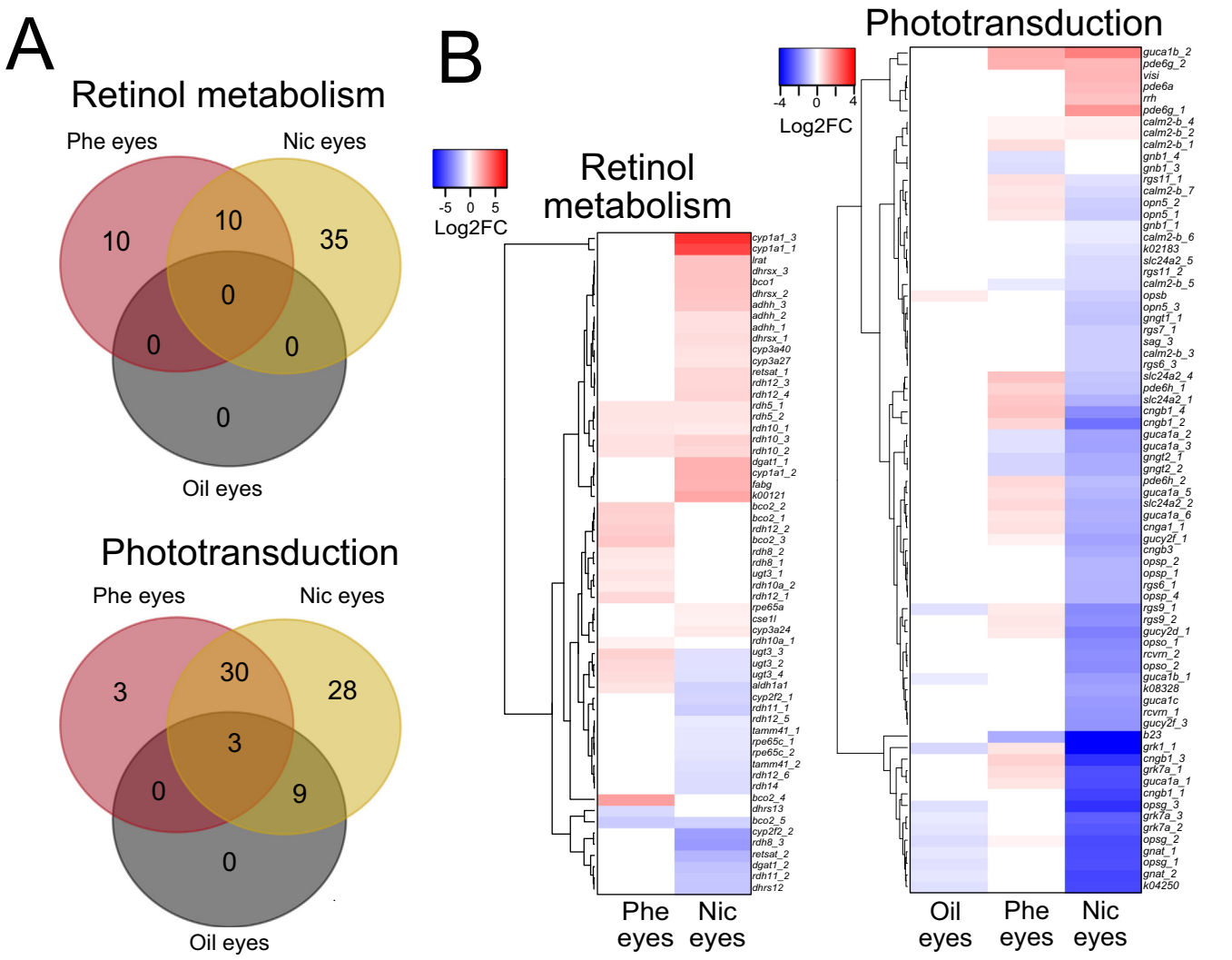

Fig. 8. Retinol metabolism and phototransduction. A) Upper: Venn diagram of differentially expressed genes (DEGs) in Retinol metabolism pathway in Phenanthrene exposed eyes (Phe eyes), Nicardipine exposed eyes (Nic eyes) and crude oil exposed eyes (Oil eyes). Lower: Venn diagram of DEGs in Phototransduction pathway in Phe exposed eyes, Nic exposed eyes and Oil exposed eyes at 3 dph. B) Heatmap of DEGs for the various exposures in Retinol metabolism pathway and Phototransduction. Gene with ID K00121 was not annotated to genebank but corresponds to ADHH, Alcohol dehydrogenase class 3 chain H in KEGG. Log2FC; base 2 logarithm of the fold change.

in our study. The difference in phenotype, i.e. arching spine in Oil and Nic and hunched spine in Phe exposure, could either be a product of timing of exposure or slight differences in mechanistic effect on muscular function. Similar to Nic exposure, silent heart morpholino zebrafish also possess severe jaw and spinal disorders (Incardona et al., 2004). This supports that jaw and spinal deformities are secondary to circulation, since the gene knocked out in silent heart morpholino zebrafish is the cardiac specific troponin 2 (*tnnt2*), necessary for cardiac contraction. In comparison, Nic blocks L-type channel in cardiac, smooth and skeletal muscle cells (Mittnacht et al., 2018). Thus, Nic induced disruption of skeletal muscle function is likely to cause spinal and craniofacial abnormalities. In summary, the observed jaw and spinal deformities found in our exposure are most likely due to multiple impacts including direct effect on skeletal muscle, and not only secondary to circulation disorders.

4.3. Cardiac dysfunction reduce fatty acid transport from the yolk

The fatty acid and cholesterol analysis suggested a disrupted transport of lipids from the yolk to the eye with possible implications on development. The altered lipid distribution was also reflected in the transcriptomic data, indicating activation of *Fatty acid metabolism* and *Cholesterol biosynthesis* pathways in the exposed eyes. Lipids are essential for eye development and growth (Bell et al., 1996; Koven et al., 2018). In line with other studies, n-3 PUFA, DHA (22:6 (n-3)), and the saturated fatty acids, stearic acid (18:0) and palmitic acid (16:0) accounted for the largest proportion of fatty acids (Stoknes et al., 2004). PUFAs contribute to the physical chemical properties of the cell membrane by influencing neurogenesis, neuroplasiticy, neurite growth, synaptogenesis and membrane permeability and fluidity (Saccà et al., 2018).

Long chain (LC)-PUFAs cannot be synthesized de novo in fish and must be consumed or obtained from yolk sac either intact or from a select group of precursors such as α -linolenic acid (18:3n-3) and linoleic acid (18:2n-6) (Gorusupudi et al., 2016). We observed reduction of PUFAs and especially DHA in the eyes of all exposures, a finding that was supported by the predicted decrease of the up-stream regulators DHA and HDL following IPA analysis. We also observed increased levels of SFAs and MUFAs, mainly palmitic acid, stearic acid and oleic acid. The changes in fatty acid profile and genes related to lipid metabolism suggests that the eyes are insufficiently trying to compensate for the deprivation of essential fatty acids by de novo synthesis of SFA and MUFAs and synthesis of LC-PUFAs by increasing desaturation and elongation of precursors. (Fig. 9).

Very long chain fatty acids (VLC-PUFA C_{24}-C_{38}) play important roles in eye development of fish larvae (Morais et al., 2020). The levels of

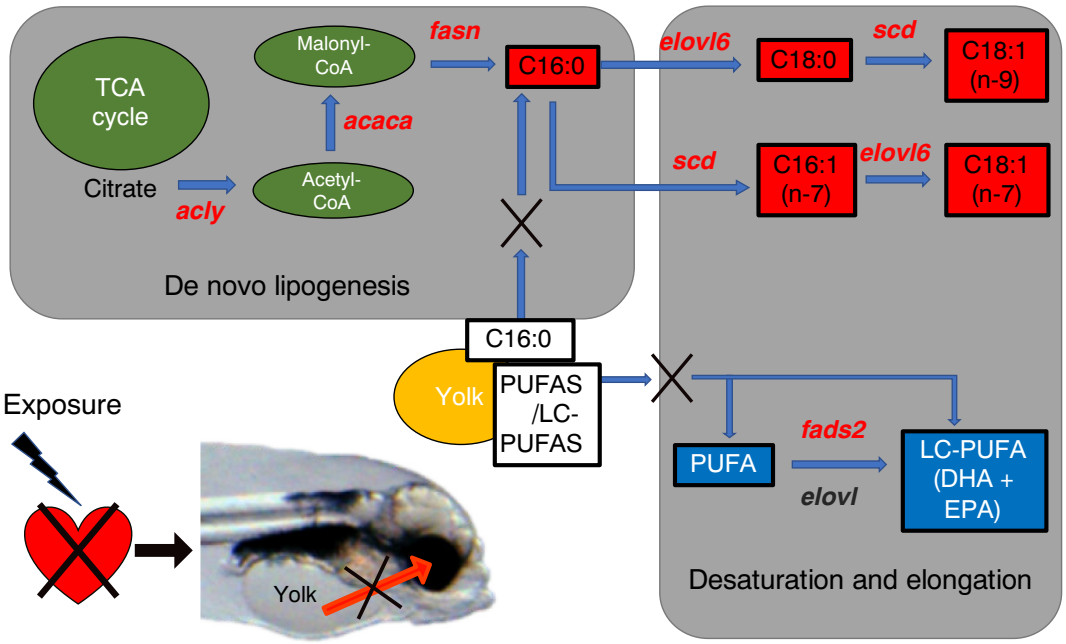

Fig. 9. Schematic overview of circulatory related effect on lipid metabolism. The data suggest that cardiac dysfunction following exposure disrupts transport of lipids from the yolk to the eye during embryonic development. As a result, increased expression of lipid metabolizing genes (red letters) in the eye facilitates de novo synthesis of saturated fatty acids (red boxes). In addition, decrease in allocation of LC-PUFAS from the yolk induces the main desaturase gene (fads2) in an effort to compensate the lack of DHA in the eye. Red and blue boxes indicate observed increase and decrease in specific fatty acids following chemical exposure (Phe and Nic). (For interpretation of the references to colour in this figure legend, the reader is referred to the web version of this article.)

these VLC-PUFAs in the organism are low, and therefore demand sensitive detection methods (Serrano et al., 2021). In present study we used conventional gas chromatography with flame ionization detector (GC-FID) and were only able to detect up to C_{24} PUFAs. But the elongase of VLC-PUFAs;C_{24}, Elovl4, which are known to be highly expressed in the eyes and brain (Agbaga et al., 2010; Morais et al., 2020), were also abundant in our eye-transcriptomes. However, *elovl4* were not up-regulated in our chemically treated groups, on the contrary two *elovl4* paralogs were down-regulated in the Nic exposure. Findings suggests that the larvae were not able to increase the synthesis of VLC-PUFAs to compensate for the reduced amount of PUFA (especially DHA) coming from the yolk.

PUFAs and cholesterol are essential for maintaining the integrity and fluidity in cell membranes (Saccà et al., 2018; Zampelas and Magriplis, 2019). A dynamic membrane composition is necessary for optimal function in varying conditions. One of the major mechanisms of maintaining membrane fluidity under changing conditions is through regulating the fatty acid groups in the membrane and cholesterol content. For example, in colder environments, enrichment of unsaturated fatty acids, such as DHA, was observed (Wallaert and Babin, 1994). Incorporation of lipophilic oil components into the membrane are proposed to impact the fluidity of the membrane and possibly alter membrane protein functions (Broniatowski et al., 2017). A recent study showed that pretreatment with cholesterol partially mitigated the effect of Phe on heart rate (McGruer et al., 2021). Although most genes in the cholesterol biosynthesis pathway were upregulated by both Nic and Phe, the rate limiting enzymes, 3-hydroxy-3-methylglutaryl-CoA reductase (*hmgcr*) and 3-hydroxy-3- methylglutaryl-CoA Synthase 1 (*hmgcs1*) were only up-regulated in Phe exposed eyes. In vitro studies show that Phe has the ability to incorporate into the cell membrane and increase the fluidity (Holmstrup et al., 2014; Liland et al., 2014). Likewise, exposure to alkyl phenols and estrogen altered the fatty acid profile to contain more SFA and less n-3 PUFA in cod (*Gadus morhua*) (Meier et al., 2007). The changes in lipid profile in our exposures could also indicate a compensatory response to altered membrane fluidity. Accordingly, we observed up-regulation of a protein that regulates fluidity of the plasma membrane (*tlcd1*). A plausible mode of action for disruption of potassium and calcium channels could be alteration of the channel by disturbing the fluidity around the channel.

To summarize the effects regarding lipids in the eyes, we observed a decrease of total fatty acids, cholesterol, and PUFAs. With this, we observed increased activation of fatty acid metabolism and cholesterol biosynthesis. All these effects could be due to a) a circulation-dependent deprivation of lipids and cholesterol, and b) compensatory response to increased cell membrane fluidity.

4.4. Calcium signaling and muscular function

Enriched pathways in 3 dph eyes of Phe and Nic exposure included signaling pathways and muscular function pathways, confirming the consequences of an impact on essential ion currents in muscle cells of the eyes. However, opposite z-activation score in the two exposures suggest an opposite cellular effect. Nic reduces cytoplasmic calcium by reducing influx of extracellular calcium, but also inhibits ion control gating mechanisms and possibly interfere with release of calcium from sarcoplasmic reticulum (Drugbank.com, 2020; Mittnacht et al., 2018). An opposite z-activation score was observed in the Phe exposure, suggesting that Phe increases intracellular calcium. Accordingly, increased intracellular calcium was also observed in rat embryonic cardiac myoblasts (H9C2) exposed to Phe (Zhang et al., 2013). The regulation of the gene *itpr1* is indicative of the opposite effect on calcium homeostasis in Nic and Phe exposure. Itpr1 controls the calcium induced calcium release (CICR) of calcium from the endoplasmic reticulum (ER) to the cytoplasm (Roderick et al., 2003). Increase of calcium in the cytoplasm induces release of more calcium to the cytoplasm from internal storages such as ER. Accordingly, we observed up-regulation of *itpr1* in Phe exposed eyes and down-regulation in Nic.

Several of the genes involved in *Calcium signaling* pathway were also represented in *Motor dysfunction or movement disorders* and *Formation of muscle* in the various exposures suggesting detection of down-

stream effects on muscular function and development in the exposures. Particularly in the Oil exposure, we mainly expected to detect gene expression linked to the down-stream effects of an oil exposure during early embryonic development. For example, only two genes were exclusive for *Calcium signaling*, while 5, 13 and 3 were exclusive for *Cardiac hypertrophy signaling*, *Motor dysfunction or movement disorders* and *Formation of muscle*, respectively. Overall, we suggest that an impact on calcium homeostasis induced muscular dysfunction and abnormal eye muscle development in the exposures. Regardless of the direction of impact on signaling pathways in Phe and Nic exposed eyes, the consequences for muscle development were similar.

4.5. Impact on eye development and vision

Based on the transcriptomic changes in *Phototransduction pathway*, our data suggest that the animals treated with Oil or Nic during early development may have resulted in blindness or reduced vision. In contrast, exposure with Phe in late embryonic development appeared to result in a more compensatory response. In Phe exposed eyes, eye development and function were likely affected by deprivation of essential nutrients and disruption of retinol metabolism. The retina of the eye is highly enriched with LC-PUFAs, and are essential for eye development (Tanito et al., 2009). PUFAs inhibit the expression of fatty acid desaturase 2 (*fads2*) and elongation of long-chain fatty acids family member 6 (*elovl6*) (Matsuzaka and Shimano, 2009; Ralston et al., 2015). An up-regulation of *fads2* and *elovl6* suggest reduced amount of PUFAs in Phe and Nic exposed eyes. Accordingly, less n-3 PUFAs (DHA) were observed in the eyes of all exposures compared to control. Due to their critical function, PUFAs in the yolk are reserved for development and not consumed for energy (Kamler, 2008). However, with circulatory defects in Phe and Nic exposed eyes, the essential PUFAs may not reach their destination and therefore could result in impaired eye development.

Retinol, often referred to as vitamin A, is a precursor for a range of biological active metabolites including vision, limb patterning, growth and normal cell homeostasis (Ross et al., 2000). The active metabolite of retinol, retinoic acid, is a known teratogen and disruption of retinoid signaling, has been shown to cause developmental abnormalities (Alsop et al., 2004; Le et al., 2012). Increased retinoic acid levels and disrupted retinoid signaling has been linked to eye deformities in crude oil exposed animals (Lie et al., 2019). Retinol metabolism in the eyes was affected by both Nic and Phe exposure, no DEGs involved in Retinol metabolism were found in Oil exposed eyes 10 days after end of exposure. Transcriptomic changes were evaluated during exposure in a previous study, and oil induced expression of *rdh8* was seen at 6 dpf (Lie et al., 2019). Up-regulation of *rdh8* was also observed in the Phe exposed eyes, suggesting acute disturbance of retinol metabolism in the Phe exposure. Imbalance of the cytochrome P450 (Cyp)-system can also disrupt retinoic acid signaling pathway, and consequently lead to abnormal eye development (Lie et al., 2019; Yamamoto et al., 2000). Cyp1a is believed to be one of the most important factors disrupting retinoid signaling following toxicant exposure (Berntssen et al., 2015; Murphy et al., 2007), and is the main gene induced in crude oil exposed animals (Sørhus et al., 2021). Another Cyp1 paralog, Cyp1b, is also involved in eye development (regulating ocular fissure closure) through both retinoic acid-dependent and -independent pathways (Chambers et al., 2007; Williams et al., 2017) and were thought to partly induce the stage dependent eye abnormalities found in Sørhus et al., 2021 (Sørhus et al., 2021). Cyp1b induction could also explain the increased levels of retinoic acid observed in conjunction with eye deformities in our previous study (Lie et al., 2019). Phe is known to be a poor inducer of Cyp1a (Hawkins et al., 2002), and Phe exposed eyes did not show any effect on any *cyp*s except *cyp51*. However, Nic exposed eyes showed induced expression of both *cyp1a* and *cyp1b* which could contribute to the observed abnormal eye development in this exposure.

In the phototransduction pathway several functional units found in photoreceptor cells (e.g. *opsg*, *opsb*) (Terakita, 2005) or genes encoding proteins involved in signal transduction (e.g. *gnat* and *rgs9*) (Burns and Pugh, 2009) were down-regulated in Oil and Nic exposed eyes. Phe exposed eyes on the other hand, showed an up-regulation of several genes involved in *Phototransduction*. In haddock embryos, *Synaptic vesicle cycle* were among most regulated pathways between 6 and 8 dpf, while *Phototransduction* was among most regulated pathways between 10 dpf and hatching (Sørhus et al., 2016a). We therefore suggest that exposure during early embryonic development (Oil and Nic) affects eye development and results in reduced vision or blindness later in life, while a late embryonic exposure mainly impact phototransduction and therefore results in a compensatory response like the one observed in Phe exposed eyes. In conclusion, we suggest a double impact on eye development and phototransduction in our exposures. Inappropriate cardiac function could lead to inadequate supply of essential fatty acids necessary for proper eye development and function and affect transport of other nutrients, such as retinoids. Additionally, disturbance of signaling in pathways such as *Retinol metabolism* may lead to abnormal eye development.

5. Conclusion

The present study was designed to identify underlying mechanisms causing the eye malformations following exposure to chemicals that disrupt cardiac function. Exposure with Oil, Phe and the L-type channel blocker Nic lead to severe eye, jaw and spinal deformities. In addition, cardiac malfunctioning was observed in Phe and Nic treated animals. Nic blocks L-type channel in all muscle tissues. Therefore, the spinal and jaw abnormalities in Nic treated animals were most likely due to disrupted muscular function and not only lack of circulation. The Nic phenotypes resembled phenotypes found in Oil and Phe exposure, thus, we suggest that a direct effect on skeletal muscle function also could be the underlying mechanism of the jaw and spinal abnormalities found in these larvae.

The lipid profile was altered in all three exposures. All exposures showed a decrease of total fatty acids, cholesterol and PUFAs and an increase of SFA and MUFAs in the eyes. Accordingly, the exposures showed high impact on cholesterol biosynthesis and fatty acid metabolism. This observation could reflect both disrupted transport of nutrients from the yolk to the eyes due to dysfunctional circulation and compensatory responses to changes in membrane fluidity. Further, the eye transcriptome of the Phe and Nic suggested an opposite effect on calcium homoeostasis in these exposures. Phe exposure likely resulted in an increase of intracellular calcium, while Nic exposure resulted in a decrease. This in turn led to opposite impact on muscle function, but down-stream effect on muscular development was the same. Our data suggest that dysfunctional and abnormal eyes in our exposures were due to both disruption of signaling and insufficient supply of essential fatty acids and other nutrients form the yolk.

Supplementary data to this article can be found online at https://doi.org/10.1016/j.scitotenv.2021.149460.

CRediT authorship contribution statement

ES: Conceptualization, Methodology, Investigation, Formal analysis, Data curation, Writing – original draft. CED: Formal analysis, Data curation, Review of paper. SM: Conceptualization, Methodology, Formal analysis, Data curation, Review of paper. TF: Methodology, Resources, Data curation, Review of paper. RBE: Methodology, Resources, Data curation, Review of paper. KKL: Investigation, Formal analysis, Data curation, Writing – original draft.

Declaration of competing interest

The authors declare no competing interests.

Acknowledgments

We would like to acknowledge Stig Ove Utskot for breeding and management of the fish, Therese Aase and Arve Fossen for carrying out the lipid analysis and Holly Shiels for discussions of the idea and interpretation of some of the data. This work was financed by the Research Council of Norway (EGGTOX: Unraveling the mechanistic effects of crude oil toxicity during early life stages of cold-water marine teleosts (Project # 267820, www.forskningsradet.no) and the Institute of Marine Research, Norway. The funders had no role in study design, data collection and analysis, decision to publish, or preparation of the manuscript.

References

Agbaga, M.P., Mandal, M.N., Anderson, R.E., 2010. Retinal very long-chain PUFAs: new insights from studies on ELOVL4 protein. J. Lipid Res. 51, 1624–1642.
Ainerua, M.O., Tinwell, J., Kompella, S.N., Sørhus, E., White, K.N., van Dongen, B.E., Shiels, H.A., 2020. Understanding the cardiac toxicity of the anthropogenic pollutant phenanthrene on the freshwater indicator species, the brown trout (Salmo trutta): from whole heart to cardiomyocytes. Chemosphere 239, 124608.
Alsop, D.H., Brown, S.B., van der Kraak, G.J., 2004. Dietary retinoic acid induces hindlimb and eye deformities in Xenopus laevis. Environ. Sci. Technol. 38, 6290–6299.
Bell, M.V., Mcevoy, L.A., Navarro, J.C., 1996. Deficit of didocosahexaenoyl phospholipid in the eyes of larval sea bass fed an essential fatty acid deficient diet. J. Fish Biol. 49, 941–952.
Berntssen, M.H.G., Ørnsrud, R., Hamre, K., Lie, K.K., 2015. Polyaromatic hydrocarbons in aquafeeds, source, effects and potential implications for vitamin status of farmed fish species: a review. Aquac. Nutr. 21, 257–273.
Berntssen, M.H.G., Ornsrud, R., Rasinger, J., Softeland, L., Lock, E.J., Kolas, K., Moren, M., Hylland, K., Silva, J., Johansen, J., Lie, K., 2016. Dietary vitamin a supplementation ameliorates the effects of poly-aromatic hydrocarbons in Atlantic salmon (Salmo salar). Aquat. Toxicol. 175, 171–183.
Brette, F., Machado, B., Cros, C., Incardona, J.P., Scholz, N.L., Block, B.A., 2014. Crude oil impairs cardiac excitation-contraction coupling in fish. Science 343, 772–776.
Brette, F., Shiels, H.A., Galli, G.L., Cros, C., Incardona, J.P., Scholz, N.L., Block, B.A., 2017. A novel cardiotoxic mechanism for a pervasive global pollutant. Sci. Rep. 7, 41476.
Broniatowski, M., Binczycka, M., Wojcik, A., Flasinski, M., Wydro, P., 2017. Polycyclic aromatic hydrocarbons in model bacterial membranes - langmuir monolayer studies. Bba-Biomembranes 1859, 2402–2412.
Burns, M.E., Pugh Jr., E.N., 2009. RGS9 concentration matters in rod phototransduction. Biophys. J. 97, 1538–1547.
Chambers, D., Wilson, L., Maden, M., Lumsden, A., 2007. RALDH-independent generation of retinoic acid during vertebrate embryogenesis by CYP1B1. Development 134, 1369–1383.
Cresci, A., Browman, H.I., Skiftesvik, A.B., Shema, S., Bjelland, R., Durif, C., Foretich, M., Di Persia, C., Lucchese, V., Vikebø, F., Sorhus, E., 2020. Effects of exposure to low concentrations of oil on expression of cytochrome P4501a and routine swimming speed of Atlantic haddock (Melanogrammus aeglefinus) larvae in situ. Environ. Sci. Technol.
Cvekl, A., Wang, W.-L., 2009. Retinoic acid signaling in mammalian eye development. Exp. Eye Res. 89, 280–291.
Drugbank.com, 2020. Nicardipine. Drugbank, https://go.drugbank.com/drugs/DB00622
Ehab, A.-M., Holly, A.S., Yihong, Z., Chunyun, D., Oliver, H., Stephen, C.H., Christopher, E.D., Jules, H., 2021. Cell Mol. Life Sci.
Gardner, L.D., Peck, K.A., Goetz, G.W., Linbo, T.L., Cameron, J.R., Scholz, N.L., Block, B.A., Incardona, J.P., 2019. Cardiac remodeling in response to embryonic crude oil exposure involves unconventional NKX family members and innate immunity genes. J. Exp, Biol, p. 222.
Goodman, C.A., Hornberger, T.A., Robling, A.G., 2015. Bone and skeletal muscle: key players in mechanotransduction and potential overlapping mechanisms. Bone 80, 24–36.
Gorusupudi, A., Liu, A., Hageman, G.S., Bernstein, P.S., 2016. Associations of human retinal very long-chain polyunsaturated fatty acids with dietary lipid biomarkers. J. Lipid Res. 57, 499–508.
Hall, T.E., Smith, P., Johnston, I.A., 2004. Stages of embryonic development in the Atlantic cod Gadus morhua. J. Morphol. 259, 255–270.
Hanna, E.M., Zhang, X., Eide, M., Fallahi, S., Furmanek, T., Yadetie, F., Zielinski, D.C., Goksøyr, A., Jonassen, I., 2020. ReCodLiver0.9: overcoming challenges in genome-scale metabolic reconstruction of a non-model species. Front. Mol. Biosci. 7, 591406.
Hawkins, S.A., Billiard, S.M., Tabash, S.P., Brown, R.S., Hodson, P.V., 2002. Altering cytochrome P4501A activity affects polycyclic aromatic hydrocarbon metabolism and toxicity in rainbow trout (Oncorhynchus mykiss). Environ. Toxicol. Chem. 21, 1845–1853.
Heintz, R.A., Short, J.W., Rice, S.D., 1999. Sensitivity of fish embryos to weathered crude oil: part II. increased mortality of pink salmon (Oncorhynchus gorbuscha) embryos incubating downstream from weathered exxon Valdez crude oil. Environ. Toxicol. Chem. 18, 494–503.
Hoehne-Reitan, K., Kjørsvik, E., 2004. Functional development of the liver and exocrine pancreas. Am. Fish. Soc. Symp. 40, 9–36.
Holmstrup, M., Bouvrais, H., Westh, P., Wang, C., Slotsbo, S., Waagner, D., Enggrob, K., Ipsen, J.H., 2014. Lipophilic contaminants influence cold tolerance of invertebrates through changes in cell membrane fluidity. Environ. Sci. Technol. 48, 9797–9803.
Incardona, J.P., Scholz, N.L., 2016. The influence of heart developmental anatomy on cardiotoxicity-based adverse outcome pathways in fish. Aquat. Toxicol. 177, 515–525.
Incardona, J.P., Collier, T.K., Scholz, N.L., 2004. Defects in cardiac function precede morphological abnormalities in fish embryos exposed to polycyclic aromatic hydrocarbons. Toxicol. Appl. Pharmacol. 196, 191–205.
Incardona, J.P., Carls, M.G., Holland, L., Linbo, T.L., Baldwin, D.H., Myers, M.S., Peck, K.A., Tagal, M., Rice, S.D., Scholz, N.L., 2015. Very low embryonic crude oil exposures cause lasting cardiac defects in salmon and herring. Sci. Rep. 5, 13499.
Kamler, E., 2008. Resource allocation in yolk-feeding fish. Rev. Fish Biol. Fisher. 18, 143–200.
Knight, R.D., Schilling, T.F., 2006. Cranial neural crest and development of the head skeleton. Adv. Exp. Med. Biol. 589, 120–133.
Koide, Y., Kimura, S., Tada, R., Kugai, N., Yamashita, K., 1983. Activation of glycogenolysis by the reduction in the extracellular calcium-concentration in verapamil-perfused rat-liver. Biochem. Pharmacol. 32, 517–522.
Kompella, S.N., Brette, F., Hancox, J.C., Shiels, H.A., 2021. Phenanthrene impacts zebrafish cardiomyocyte excitability by inhibiting I-kr and shortening action potential duration. J. Gen, Physiol, p. 153.
Koven, W., Nixon, O., Allon, G., Gaon, A., El Sadin, S., Falcon, J., Besseau, L., Escande, M., Vassallo Agius, R., Gordin, H., Tandler, A., 2018. The effect of dietary DHA and taurine on rotifer capture success, growth, survival and vision in the larvae of Atlantic bluefin tuna (Thunnus thynnus). Aquaculture 482, 137–145.
Langmead, B., Trapnell, C., Pop, M., Salzberg, S.L., 2009. Ultrafast and memory-efficient alignment of short DNA sequences to the human genome. Genome Biol. 10.
Le, H.G., Dowling, J.E., Cameron, D.J., 2012. Early retinoic acid deprivation in developing zebrafish results in microphthalmia. Vis. Neurosci. 29, 219–228.
Lie, K.K., Meier, S., Sørhus, E., Edvardsen, R.B., Karlsen, O., Olsvik, P.A., 2019. Offshore crude oil disrupts retinoid signaling and eye development in larval Atlantic haddock. Front. Mar, Sci, p. 6.
Liland, N.S., Simonsen, A.C., Duelund, L., Torstensen, B.E., Berntssen, M.H., Mouritsen, O.G., 2014. Polyaromatic hydrocarbons do not disturb liquid-liquid phase coexistence, but increase the fluidity of model membranes. Chem. Phys. Lipids 184, 18–24.
Magnuson, J.T., Khursigara, A.J., Allmon, E.B., Esbaugh, A.J., Roberts, A.P., 2018. Effects of Deepwater horizon crude oil on ocular development in two estuarine fish species, red drum (Sciaenops ocellatus) and sheepshead minnow (Cyprinodon variegatus). Ecotoxicol. Environ. Saf. 166, 186–191.
Marris, C.R., N., K.S., Miller, M.R., Incardona, J.P., Brette, F., C., H.J., Sørhus, E., Shiels, H.A., 2019. Polyaromatic hydrocarbons in pollution: a heart-breaking matter. J. Physiol. 598, 227–247.
Matsuzaka, T., Shimano, H., 2009. Elovl6: a new player in fatty acid metabolism and insulin sensitivity. J. Mol. Med. 87, 379–384.
McGruer, V., Tanabe, P., Vliet, S.M.F., Dasgupta, S., Qian, L., Volz, D.C., Schlenk, D., 2021. Effects of phenanthrene exposure on cholesterol homeostasis and cardiotoxicity in zebrafish embryos. Environ. Toxicol. Chem.
Meier, S., Mjos, S.A., Joensen, H., Grahl-Nielsen, O., 2006. Validation of a one-step extraction/methylation method for determination of fatty acids and cholesterol in marine tissues. J. Chromatogr. A 1104, 291–298.
Meier, S., Andersen, T.C., Lind-Larsen, K., Svardal, A., Holmsen, H., 2007. Effects of alkylphenols on glycerophospholipids and cholesterol in liver and brain from female Atlantic cod (Gadus morhua). Comp. Biochem. Physiol. C Toxicol. Pharmacol. 145, 420–430.
Mittnacht, A.J.C., London, M.J., Puskas, J.D., Kaplan, J.A., 2018. Chapter 14 - anesthesia for myocardial revascularization. In: Kaplan, J.A. (Ed.), Kaplan's Essentials of Cardiac Anesthesia, Second edition Elsevier, Philadelphia, pp. 322–351.
Morais, S., Torres, M., Hontoria, F., Monroig, Ó., Varó, I., Agulleiro, M.J., Navarro, J.C., 2020. Molecular and functional characterization of Elovl4 genes in Sparus aurata and Solea senegalensis pointing to a critical role in very long-chain (>C(24)) fatty acid synthesis during early neural development of fish. Int. J. Mol, Sci, p. 21.
Murphy, K.A., Quadro, L., White, L.A., 2007. The intersection between the aryl hydrocarbon receptor (AhR)- and retinoic acid-signaling pathways. Vitam. Horm. 75, 33–67.
Newton, A.C., Bootman, M.D., Scott, J.D., 2016. Second messengers. Cold Spring Harb. Perspect, Biol, p. 8.
Perrichon, P., Mager, E.M., Pasparakis, C., Stieglitz, J.D., Benetti, D.D., Grosell, M., Burggren, W.W., 2018. Combined effects of elevated temperature and Deepwater horizon oil exposure on the cardiac performance of larval mahi-mahi. Coryphaena hippurus, Plos One, p. 13.
Perrichon, P., Donald, C.E., Sørhus, E., Harboe, T., Meier, S., 2021. Differential developmental toxicity of crude oil in early life stages of Atlantic halibut (Hippoglossus hippoglossus). Sci. Total Environ. 770, 145349.
Planchart, A., Mattingly, C.J., 2010. 2,3,7,8-tetrachlorodibenzo-p-dioxin upregulates FoxQ1b in zebrafish jaw primordium. Chem. Res. Toxicol. 23, 480–487.
R Core Team, 2013. R: A Language and Environment for Statistical Computing. R Foundation for Statistical Computing, Vienna, Austria. Retrieved from: https://www.R-project.org.
Ralston, J.C., Matravadia, S., Gaudio, N., Holloway, G.P., Mutch, D.M., 2015. Polyunsaturated fatty acid regulation of adipocyte FADS1 and FADS2 expression and function. Obesity 23, 725–728.
Roderick, H.L., Berridge, M.J., Bootman, M.D., 2003. Calcium-induced calcium release. Curr. Biol. 13, R425.
Ross, S.A., McCaffery, P.J., Drager, U.C., De Luca, L.M., 2000. Retinoids in embryonal development. Physiol. Rev. 80, 1021–1054.

Saccà, S.C., Cutolo, C.A., Ferrari, D., Corazza, P., Traverso, C.E., 2018. The eye, oxidative damage and polyunsaturated fatty acids. Nutrients 10, 668.
Sato, Y., Fujino, M., 1987. Inhibition of excitation-contraction coupling by a ca channel blocker nicardipine at low-temperature in frog twitch fibers. Jpn. J. Physiol. 37, 93–108.
Schneider, C.A., Rasband, W.S., Eliceiri, K.W., 2012. NIH Image to ImageJ: 25 years of image analysis. Nat. Methods 9, 671–675.
Serrano, R., Navarro, J.C., Portolés, T., Sales, C., Beltrán, J., Monroig, Ó., Hernández, F., 2021. Identification of new, very long-chain polyunsaturated fatty acids in fish by gas chromatography coupled to quadrupole/time-of-flight mass spectrometry with atmospheric pressure chemical ionization. Anal. Bioanal. Chem. 413, 1039–1046.
Shwartz, Y., Farkas, Z., Stern, T., Aszodi, A., Zelzer, E., 2012. Muscle contraction controls skeletal morphogenesis through regulation of chondrocyte convergent extension. Dev. Biol. 370, 154–163.
Sørensen, L., Meier, S., Mjøs, S.A., 2016. Application of gas chromatography/tandem mass spectrometry to determine a wide range of petrogenic alkylated polycyclic aromatic hydrocarbons in biotic samples. Rapid Commun Mass Sp 30, 2052–2058.
Sørensen, L., Sørhus, E., Nordtug, T., Incardona, J.P., Linbo, T.L., Giovanetti, L., Karlsen, O., Meier, S., 2017. Oil droplet fouling and differential toxicokinetics of polycyclic aromatic hydrocarbons in embryos of Atlantic haddock and cod. Plos One 12, e0180048.
Sørensen, L., McCormack, P., Altin, D., Robson, W.J., Booth, A.M., Faksness, L.G., Rowland, S.J., Størseth, T.R., 2019. Establishing a link between composition and toxicity of offshore produced waters using comprehensive analysis techniques - a way forward for discharge monitoring? Sci. Total Environ. 694, 133682.
Sørhus, E., Edvardsen, R.B., Karlsen, O., Nordtug, T., van der Meeren, T., Thorsen, A., Harman, C., Jentoft, S., Meier, S., 2015. Unexpected interaction with dispersed crude oil droplets drives severe toxicity in Atlantic haddock embryo. Plos One 10, e0124376.
Sørhus, E., Incardona, J.P., Furmanek, T., Jentoft, S., Meier, S., Edvardsen, R.B., 2016a. Developmental transcriptomics in Atlantic haddock: illuminating pattern formation and organogenesis in non-model vertebrates. Dev. Biol. 411, 301–313.
Sørhus, E., Incardona, J.P., Karlsen, O., Linbo, T., Sørensen, L., Nordtug, T., van der Meeren, T., Thorsen, A., Thorbjørnsen, M., Jentoft, S., Edvardsen, R.B., Meier, S., 2016b. Crude oil exposures reveal roles for intracellular calcium cycling in haddock craniofacial and cardiac development. Sci. Rep. 6, 31058.
Sørhus, E., Incardona, J.P., Furmanek, T., Goetz, G.W., Scholz, N.L., Meier, S., Edvardsen, R.B., Jentoft, S., 2017. Novel adverse outcome pathways revealed by chemical genetics in a developing marine fish. elife 6.
Sørhus, E., Donald, C.E., da Silva, D., Thorsen, A., Karlsen, Ø., Meier, S., 2021. Untangling mechanisms of crude oil toxicity: linking gene expression, morphology and PAHs at two developmental stages in a cold-water fish. Sci. Total Environ. 757, 143896.
Star, B., Nederbragt, A.J., Jentoft, S., Grimholt, U., Malmstrom, M., Gregers, T.F., Rounge, T.B., Paulsen, J., Solbakken, M.H., Sharma, A., Wetten, O.F., Lanzen, A., Winer, R., Knight, J., Vogel, J.H., Aken, B., Andersen, O., Lagesen, K., Tooming-Klunderud, A., Edvardsen, R.B., Tina, K.G., Espelund, M., Nepal, C., Previti, C., Karlsen, B.O., Moum, T., Skage, M., Berg, P.R., Gjoen, T., Kuhl, H., Thorsen, J., Malde, K., Reinhardt, R., Du, L., Johansen, S.D., Searle, S., Lien, S., Nilsen, F., Jonassen, I., Omholt, S.W., Stenseth, N.C., Jakobsen, K.S., 2011. The genome sequence of Atlantic cod reveals a unique immune system. Nature 477, 207–210.
Stifani, N., 2014. Motor neurons and the generation of spinal motor neuron diversity. Cell Neurosci. 8, 1–22.
Stoknes, I.S., Økland, H.M., Falch, E., Synnes, M., 2004. Fatty acid and lipid class composition in eyes and brain from teleosts and elasmobranchs. Comp. Biochem. Physiol. B Biochem. Mol. Biol. 138, 183–191.
Tanito, M., Brush, R.S., Elliott, M.H., Wicker, L.D., Henry, K.R., Anderson, R.E., 2009. High levels of retinal membrane docosahexaenoic acid increase susceptibility to stress-induced degeneration. J. Lipid Res. 50, 807–819.
Terakita, A., 2005. The opsins. Genome Biol. 6, 213.
Vergauwen, L., Schmidt, S.N., Stinckens, E., Maho, W., Blust, R., Mayer, P., Covaci, A., Knapen, D., 2015. A high throughput passive dosing format for the fish embryo acute toxicity test. Chemosphere 139, 9–17.
Wallaert, C., Babin, P.J., 1994. Thermal adaptation affects the fatty acid composition of plasma phospholipids in trout. Lipids 29, 373–376.
Wasta, Z., Mjøs, S.A., 2013. A database of chromatographic properties and mass spectra of fatty acid methyl esters from omega-3 products. J. Chromatogr. A 1299, 94–102.
Williams, A.L., Eason, J., Chawla, B., Bohnsack, B.L., 2017. Cyp1b1 regulates ocular fissure closure through a retinoic acid-independent pathway. Invest. Ophth. Vis, Sci, p. 58.
Xiong, K.M., Peterson, R.E., Heideman, W., 2008. Aryl hydrocarbon receptor-mediated Down-regulation of Sox9b causes jaw malformation in zebrafish embryos. Mol. Pharmacol. 74, 1544–1553.
Yamamoto, Y., Zolfaghari, R., Ross, A.C., 2000. Regulation of CYP26 (cytochrome P450RAI) mRNA expression and retinoic acid metabolism by retinoids and dietary vitamin a in liver of mice and rats. FASEB J. 14, 2119–2127.
Zampelas, A., Magriplis, E., 2019. New insights into cholesterol functions: a friend or an Enemy? Nutrients 11.
Zhang, Y.Y., Huang, L.X., Zuo, Z.H., Chen, Y.X., Wang, C.G., 2013. Phenanthrene exposure causes cardiac arrhythmia in embryonic zebrafish via perturbing calcium handling. Aquat. Toxicol. 142, 26–32.